Advances in Mathematical Sciences and Applications, 1998, Vol. 8, No. 1, pp. 455-490.

Crystalline curvature flow of a graph in a variational setting

Charles M. Elliott, Andrew R. Gardiner[1]
Centre for Mathematical Analysis and its Applications, School of Mathematical Sciences,
University of Sussex, GB-Falmer, Brighton BN1 9QH, Great Britain,
email: C.M.Elliott@sussex.ac.uk, mmff8@solx1.central.sussex.ac.uk

Reiner Schätzle[2]
Universität Bonn, Institut für Angewandte Mathematik, Wegelerstraße 6,
D-53115 Bonn, Germany, email: reiner@iam.uni-bonn.de

Abstract:
In this paper, we investigate the properties of a definition of crystalline curvature flow given recently by Fukui and Giga in [6]. This definition coincides with that given by Angenant and Gurtin in [2] and by Taylor et. al. in [12],[13] and [15] for admissible faceted curves. Our investigation is concerned with faceted curves which are not necessarily admissible Wulff curves. We prove that faceted curves remain faceted and attain a stationary state after a finite time. But the evolving curves need not become admissible Wulff curves. We introduce a scheme for the numerical computation of the evolution and visualise our results through our computations.
AMS Subject Classification: 35 R 35, 35 K 22, 35 K 65.

1 Introduction

We consider a smooth, convex surface energy density γ as in [8]. γ is homogeneous of degree one and assigns to a smooth curve r a surface energy via the integral

$$\int_r \gamma(N)\mathrm{ds},$$

where N is the normal to the curve r. The convex set $[\gamma \leq 1]$ is called the Frank-diagram of the surface energy density γ, and

$$W(\gamma) := \{y \in I\!R^2 \mid \forall x \in I\!R^2 : xy \leq \gamma(x)\ \}$$

is the Wulff-shape of γ. In the isotropic case, where no direction is preferred, γ is constant and the Wulff-shape is a circle.
We define $\tilde{\gamma}(\theta) := \gamma(\cos(\theta), \sin(\theta))$ and consider the weighted mean-curvature flow

$$V_N = -(\tilde{\gamma} + \tilde{\gamma}'')(\theta(N))\kappa, \tag{1}$$

[1]The work of A.R. Gardiner was supported by the EPSRC.
[2]The work of R. Schätzle was supported by the ESF.

where N is the normal, and $\theta(N)$ is the angle of this normal to the positive x-axis. Under this evolution the surface energy of the interface decreases. Mean-curvature and weighted mean-curvature flow for a non-smooth or singular evolution was defined by Evans and Spruck in [5] and by Chen, Giga, and Goto in [3].

Now we drop the assumptions about smoothness of γ, instead we demand that the Frank-diagram of γ is a convex polygon. Then γ is called a crystalline energy. By a duality of corners and facets the corresponding Wulff-shape is also a convex polygon. The weighted mean-curvature flow induced by γ, called crystalline curvature flow, cannot be written as in (1). Angenant and Gurtin in [2], Taylor in [12],[13] and Taylor, Cahn, and Handwerker in [15] have given a definition for crystalline curvature flow for Wulff curves that is for curves whose normal-directions of their facets occur as normal directions of facets in the Wulff-shape. Related topics are treated for example in [1],[9] and [11].
Recently, Fukui and Giga in [6] have given a definition of crystalline curvature flow for periodic graphs, and they show that in the special case when the evolution consists of Wulff curves, this definition coincides with that in [2], [12], [13] and [15]. We note that a convergence result in the case of admissible Wulff curves for crystalline curvature flow to mean-curvature flow as the Wulff-shape converges to a circle has been proved by Girão and Kohn in [7]. In this paper, we investigate this definition for general faceted curves. We introduce a numerical scheme and compute the solutions.

In section 2, we prove that faceted curves remain faceted throughout the evolution, but that non-Wulff-shape normal directions do not disappear instantly. Indeed, there are stationary states which have non-Wulff-shape facets. For faceted curves which consist only of Wulff-shape facets but violate that adjacent facets are adjacent in the Wulff-shape, we prove that facets of the missing directions are inserted instantly. We specify all faceted, stationary states and prove that the evolution attains a stationary state in finite time for all Lipschitz-continuous initial data. Also we consider in detail the evolution of a class of curves containing curved facets. A numerical scheme based on a discretisation of the nonlinear parabolic equation of Fukui and Giga is described in section 3. A convergence result as the mesh size tends to zero is proved. Finally in section 4 extensive numerical experiments illustrating the theory and other features of crystalline curvature flow are described.

2 Theoretical results

2.1 Formulation and bounds

First, we describe the definition of crystalline mean-curvature flow given by Fukui and Giga in [6] for periodic graphs in the plane. Let the graph Γ_t at time t be represented by $u(.,t) : I\!R \to I\!R$, which is periodic with period $\varrho > 0$. γ denotes the crystalline energy. γ is continuous, convex, homogeneous of degree one and positive on the unit sphere. That γ represents a crystalline energy means that the Frank diagram of γ

$$F(\gamma) := \{z \in I\!R^2 \mid \gamma(z) \leq 1 \}$$

is a convex polygon. Then the corresponding Wulff-shape defined by

$$W(\gamma) := \{w \in I\!R^2 \mid \forall z \in I\!R^2 : w\ z \leq \gamma(z) \}$$

is a convex polygon too, as can be shown. The normal directions of the facets of the Wulff-shape will be the preferred normal directions of Γ_t. The normal of Γ_t is given by $\frac{(-u_x,1)}{\sqrt{1+|u_x|^2}}$ when u

is differentiable. Therefore we consider a bijection between $\mathbb{R}$ and $S^1 \cap \{(x,y) \in \mathbb{R}^2 \mid y > 0\}$ defined by

$$p \longleftrightarrow \frac{(-p,1)}{\sqrt{1+p^2}}, \quad p \in \mathbb{R}. \tag{1}$$

As $p \to \pm\infty$ the angle of the assigned unit vector with the x-axis tends to 0 respectively to π. $p = 0$ corresponds to the angle $\frac{\pi}{2}$.
The evolution law of Fukui and Giga for Γ_t is given by

$$u_t = g(u_x)_x \tag{2}$$

where $g : \mathbb{R} \to \mathbb{R}$ is a monotone increasing, piecewise constant function with jumps at those p which correspond to normal directions of the facets of the Wulff-shape, the height of the jump given by the length of the facet. Therefore g takes the following form

$$g = \alpha_0 + \sum_{i=1}^{N} \alpha_i \chi_{]p_i,\infty[},$$

where $p_1 < \ldots < p_N$ correspond through (1) to the normal directions of the facets of the Wulff-shape and $\alpha_1, \ldots, \alpha_N > 0$ are the respective lengths of the facets in the Wulff-shape. α_0 is arbitrary. In [6], g was defined by a Riemann-Stieltjes integral for convex and Lipschitz-continuous γ. In the case where the Frank-diagram of γ is a polygon, g takes the form above.
In Fig.1 (a),(b) we display the upper parts of two Wulff-shapes corresponding to a g with jumps at -2,-1,1,2 each of length 1 in (a), and with jumps at -1,0,1 of lengths 1,2,1 in (b).

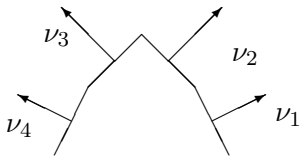

Fig.1 (a)

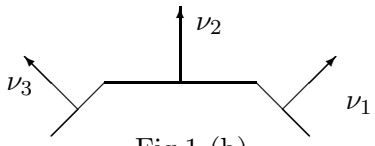

Fig.1 (b)

Properly (2) means that the variational inequality

$$\int_0^T \int_0^\varrho u_t u + G(u_x) \leq \int_0^T \int_0^\varrho u_t \eta + G(\eta_x) \tag{3}$$

is satisfied for all periodic $\eta \in \mathrm{L}^2(0,\mathrm{T};\mathrm{H}^{1,2}(0,\varrho))$, where $G' = g$. Existence of a unique solution of (3) was proved by Fukui and Giga in [6] for given initial condition $u(.,0) = u_0$, where u_0 is Lipschitz-continuous and periodic.
We consider $g_\varepsilon \in \mathrm{C}^\infty(\mathbb{R}), \mathrm{G}'_\varepsilon = \mathrm{g}_\varepsilon$ with $\varepsilon \leq \mathrm{g}'_\varepsilon$, $|\mathrm{g}_\varepsilon| \leq \Lambda$ on $[-\frac{1}{\varepsilon}, \frac{1}{\varepsilon}]$, and $\| \mathrm{G} - \mathrm{G}_\varepsilon \|_{\mathrm{L}^\infty_{\mathrm{loc}}(\mathbb{R})} \to 0$, where $0 \leq \Lambda < \infty$. Further we choose $u_{0,\varepsilon} \in \mathrm{C}^\infty(\mathbb{R})$, periodic with $\| u_{0,\varepsilon} \|_{\mathrm{C}^{0,1}(\mathbb{R})} \leq \Lambda$ and $\| u_0 - u_{0,\varepsilon} \|_{\mathrm{L}^\infty(\mathbb{R})} \to 0$. Then the unique solution u of (3) is the limit in spaces specified below of $(u_\varepsilon)_{\varepsilon>0}$, where u_ε is the unique solution of

$$\begin{aligned} u_{\varepsilon,t} &= g_\varepsilon(u_{\varepsilon,x})_x \quad \text{in } \mathbb{R} \times [0,\infty[, \\ u_\varepsilon(.,0) &= u_{0,\varepsilon}. \end{aligned} \tag{4}$$

We get $u_\varepsilon \in \mathrm{C}^\infty(\mathbb{R} \times [0,\infty[)$, as it is easily seen. Comparing u_ε with $\| \mathrm{u}_{0,\varepsilon} \|_{\mathrm{L}^\infty(\mathbb{R})}$ and $\mathrm{u}_\varepsilon(. - \mathrm{h}, .) \pm \mathrm{h} \| \mathrm{u}_{0,\varepsilon,\mathrm{x}} \|_{\mathrm{L}^\infty(\mathbb{R})}$ we conclude

$$\| u_\varepsilon \|_{\mathrm{L}^\infty(\mathbb{R}\times[0,\infty[)}, \ \| u_{\varepsilon,x} \|_{\mathrm{L}^\infty(\mathbb{R}\times[0,\infty[)} \leq C(\Lambda). \tag{5}$$

Multiplying (4) by $u_{\varepsilon,t}$ and integrating, we get, assuming $\varrho \le \Lambda$,

$$\int_0^t \int_0^\varrho |u_{\varepsilon,t}|^2 + \int_0^\varrho G_\varepsilon(u_{\varepsilon,x}(t)) = \int_0^\varrho G_\varepsilon(u_{0,\varepsilon,x}),$$

hence

$$\int_0^\infty \int_0^\varrho |u_{\varepsilon,t}|^2 \le C(\Lambda), \tag{6}$$

for small ε . Consequently u_ε converges strongly in $\mathrm{L}^2(0,\mathrm{T};\mathrm{L}^2(0,\varrho))$, and weakly in $\mathrm{L}^2(0,\mathrm{T};\mathrm{H}^{1,2}(0,\varrho))$ to u, and $u_{\varepsilon,t}$ converges weakly in $\mathrm{L}^2(0,\mathrm{T};\mathrm{L}^2(0,\varrho))$ to $\mathrm{u_t}$. We differentiate (4) by x , write $v_\varepsilon := u_{\varepsilon,x}$, and get

$$\begin{gathered} v_{\varepsilon,t} = g_\varepsilon(v_\varepsilon)_{xx} \quad \text{in } I\!R \times [0,\infty[, \\ v_\varepsilon(.,0) = u_{0,\varepsilon,x}. \end{gathered} \tag{7}$$

From (5) we get

$$\| v_\varepsilon \|_{\mathrm{L}^\infty(I\!R\times[0,\infty[)} \le C(\Lambda). \tag{8}$$

We set $w_\varepsilon := g_\varepsilon(u_{\varepsilon,x})$ and get from (4) and (6)

$$\| w_\varepsilon \|_{\mathrm{L}^\infty(I\!R\times[0,\infty[)},\ \| w_{\varepsilon,x} \|_{\mathrm{L}^2(0,\infty;\mathrm{L}^2(0,\varrho))} \le C(\Lambda). \tag{9}$$

Finally we multiply (7) with $(w_{\varepsilon,t})\chi = g'_\varepsilon(v_\varepsilon)v_{\varepsilon,t}\chi,$ where $\chi \in \mathrm{C}^\infty([0,\mathrm{t_0}]),\ \chi(0)=0,\ 0\le\chi\le 1$. We obtain

$$\int_0^{t_0} \int_0^\varrho g'_\varepsilon(v_\varepsilon)|v_{\varepsilon,t}|^2\chi + \int_0^{t_0} \int_0^\varrho \frac{\mathrm{d}}{\mathrm{dt}}(\frac{1}{2}|w_{\varepsilon,x}|^2)\chi \le 0,$$

and, since $g'_\varepsilon \ge 0,\ \chi \ge 0,$ and $\chi(0) = 0$,

$$\int_0^\varrho |w_{\varepsilon,x}(t_0)|^2\chi(t_0) \le \int_0^{t_0} \int_0^\varrho |w_{\varepsilon,x}|^2\chi_t.$$

Choosing χ such that $\chi(t_0) = 1$ and $|\chi_t| \le \frac{2}{t_0}$, we get

$$\int_0^\varrho |w_{\varepsilon,x}(t)|^2 \le C(\Lambda)t^{-1} \quad \text{for } 0 < t < \infty. \tag{10}$$

For a subsequence w_ε has a weak limit $w \in \mathrm{L}^2(0,\mathrm{T};\mathrm{L}^2(0,\varrho))$. Passing to the limit and collecting all the bounds from above, we get defining $v := u_x$

$$\begin{aligned} u_t &= w_x, \\ v_t &= w_{xx}, \end{aligned} \tag{11}$$

and

$$\begin{gathered} \| u \|_{\mathrm{L}^\infty(I\!R\times[0,\infty[)},\ \| u_x \|_{\mathrm{L}^\infty(I\!R\times[0,\infty[)},\ \| u_t \|_{\mathrm{L}^2(0,\infty;\mathrm{L}^2(0,\varrho))}, \\ \| v \|_{\mathrm{L}^\infty(I\!R\times[0,\infty[)},\ \| w \|_{\mathrm{L}^\infty(I\!R\times[0,\infty[)},\ \| w_x \|_{\mathrm{L}^2(0,\infty;\mathrm{L}^2(0,\varrho))} \le C(\Lambda), \end{gathered} \tag{12}$$

and

$$\| w_x(t) \|_{\mathrm{L}^2(0,\varrho)} \le C(\Lambda)t^{-\frac{1}{2}}.$$

Further

$$"w \in \partial G(u_x)"$$

in some sense which is specified in the next subsection. w is given only up to a constant. Finally, since w is periodic, we get from (11) that

$$\int_0^\varrho u(.,t) = \int_0^\varrho u_0.$$

2.2 Faceted solutions

We say that Γ_t is faceted if $u_x(.,t)$ is piecewise constant. An open interval in which u_x is constant and for which u_x is discontinuous at the end points is said to be a facet. We say that a facet is a Wulff-shape facet if its normal direction is the normal direction to a facet occurring in the Wulff-shape. If all the facets of a faceted curve are Wulff-shape facets then we say the curve is a Wulff curve.

The normal directions of the Wulff-shape are supposed to be the preferred normal directions of Γ_t . One might expect the typical Γ_t would be a Wulff curve whose adjacent normal directions should be adjacent in the Wulff-shape either in the same order or reversed. But Γ_t need not attain this type instantly. Indeed, we will give examples below that non-Wulff-shape directions can stay even for the whole time of the evolution. Nevertheless the above type is very attractive for Γ_t . We will prove that Γ_t remains faceted when Γ_0 is faceted. Moreover if the normal directions of two adjacent facets of Γ_0 are not adjacent in the Wulff-shape then the evolution inserts those facets with normal directions in the Wulff-shape between the two adjacent facets, and these facets are inserted instantly. Also non-Wulff-shape facets cannot increase in length and, generally, they shrink.

We recall

$$g = \alpha_0 + \sum_{i=1}^{N} \alpha_i \chi_{]p_i,\infty[}, \tag{1}$$

where $p_1 < \ldots < p_N$ correspond through (2.1.1) to the normal directions of the facets of the Wulff-shape and $\alpha_1, \ldots, \alpha_N > 0$ are the respective lengths of the facets in the Wulff-shape. α_0 is arbitrary. We are seeking solutions of (2.1.2 - 3 - 11) which have in space piecewise constant $u_x = v$. We consider $s_i \in \mathrm{C}^0([0, \mathrm{t}_0[)$ for $i \in \mathbb{Z}$ such that

$$v(x,t) = q_i \quad \text{for } s_{i-1}(t) < x < s_i(t), \tag{2}$$

where $s_{i-1}(t) < s_i(t)$ for $t \in [0, t_0[$ and $q_i \neq q_{i+1}$ is assumed. Since v shall be periodic we assume that $q_{i+n} = q_i$ and $s_{i+n} = s_i + \varrho$, for some $n \geq 2$ so that we have a finitely faceted curve with at least two facets. Next we define $w \in g(v)$, where g is considered as a set-valued function. $g(q)$ consists of exactly one element when $q \notin \{p_1, \ldots, p_N\}$, and it is a closed interval of length α_i for $q = p_i$. First we have to demand

$$w(s_i(t), t) \in g(q_i) \cap g(q_{i+1}). \tag{3}$$

It is easily seen that $\#(g(q_i) \cap g(q_{i+1})) \leq 1$ when $q_i \neq q_{i+1}$, and $g(q_i) \cap g(q_{i+1}) \neq \emptyset$ if and only if there is a $j \in \{1, \ldots, N+1\}$ such that $p_{j-1} \leq q_i,\ q_{i+1} \leq p_j$. Here we have set $p_0 = -\infty$ and $p_{N+1} = +\infty$. At this stage we assume that adjacent slopes of u are admissible, that is

$$g(q_i) \cap g(q_{i+1}) \neq \emptyset, \tag{4}$$

and we denote the unique element of this set by $\alpha_{q_i,q_{i+1}}$. (4) reflects the above mentioned claim that adjacent normal directions in Γ_t should be adjacent in the Wulff-shape. (3) reads now

$$w(s_i(t),t) = \alpha_{q_i,q_{i+1}}. \tag{3}$$

We extend $w(.,t)$ to be periodic and continuous on $\mathbb{R}$ such that $\int_{s_i}^{s_{i+n}} |w_x|^2$ is minimized, that is $w(.,t)$ is piecewise linear or equivalently $w_{xx}(.,t) = 0$ on $]s_{i-1}(t), s_i(t)[$. Therefore

$$w_x(x,t) = \frac{\alpha_{q_i,q_{i+1}} - \alpha_{q_{i-1},q_i}}{s_i(t) - s_{i-1}(t)} \quad \text{for } s_{i-1}(t) < x < s_i(t). \tag{5}$$

Next we derive a system of ordinary differential equations for $\{s_i\}$ assuming that s_i is differentiable. We choose $s_{i-1}(t) < \beta^- < s_i(t) < \beta^+ < s_{i+1}(t)$ and compute

$$\int_{\beta^-}^{\beta^+} v = (s_i(t) - \beta^-)q_i + (\beta^+ - s_i(t))q_{i+1},$$

hence

$$\frac{\mathrm{d}}{\mathrm{dt}} \int_{\beta^-}^{\beta^+} v = s_i'(t)(q_i - q_{i+1}).$$

Further, using (5),

$$\int_{\beta^-}^{\beta^+} w_{xx}(.,t) = w_x(\beta^+,t) - w_x(\beta^-,t) = \frac{\alpha_{q_{i+1},q_{i+2}} - \alpha_{q_i,q_{i+1}}}{s_{i+1}(t) - s_i(t)} - \frac{\alpha_{q_i,q_{i+1}} - \alpha_{q_{i-1},q_i}}{s_i(t) - s_{i-1}(t)}.$$

Requiring $v_t = w_{xx}$ in the sense of distributions, see (2.1.11) yields

$$s_i'(t) = \frac{1}{q_i - q_{i+1}}\left(\frac{\alpha_{q_{i+1},q_{i+2}} - \alpha_{q_i,q_{i+1}}}{s_{i+1}(t) - s_i(t)} - \frac{\alpha_{q_i,q_{i+1}} - \alpha_{q_{i-1},q_i}}{s_i(t) - s_{i-1}(t)}\right). \tag{6}$$

These equations are supplemented by the initial conditions

$$s_i(0) = s_{i,0},$$

where $s_{i-1,0} < s_{i,0}$ and $s_{i+n,0} = s_{i,0} + \varrho$ is assumed. Taking into account that $q_{i+n} = q_i$, standard theory of ordinary differential equations gives the existence of a unique solution $s_i \in \mathrm{C}^1([0, \mathrm{t}_0[)$ to (6). Moreover we take $0 < t_0 \leq \infty$ such that $[0, t_0[$ is the maximal interval of the solution.

Now we assume that $\{s_i\}$, w_x, and v are defined by (6),(5), and (2), and show that $v_t = w_{xx}$. Take $\eta \in \mathrm{C}_0^\infty(]\beta^-, \beta^+[)$. We obtain

$$-\int_{\beta^-}^{\beta^+} w_x \eta_x = \eta(s_i(t))(w_x(s_i(t)+,t) - w_x(s_i(t)-,t)) = \eta(s_i(t))(q_i - q_{i+1})s_i'(t) \tag{7}$$

with (5) and (6).
For $\eta \in \mathrm{C}_0^\infty(]\beta^-, \beta^+[\times \mathrm{U(t)})$, where $U(t)$ is some neighbourhood of t , we get

$$\int_{\beta^-}^{\beta^+} v\eta = \int_{\beta^-}^{s_i(t)} q_i\eta + \int_{s_i(t)}^{\beta^+} q_{i+1}\eta$$

and

$$\frac{\mathrm{d}}{\mathrm{dt}} \int_{\beta^-}^{\beta^+} v\eta = \eta(s_i(t),t)(q_i - q_{i+1})s_i'(t) + \int_{\beta^-}^{\beta^+} v\eta_t =$$
$$= -\int_{\beta^-}^{\beta^+} w_x\eta_x + \int_{\beta^-}^{\beta^+} v\eta_t$$

with (7). For periodic $\eta \in \mathrm{C}^\infty(I\!R \times [0,\mathrm{T}])$, $\eta(\mathrm{T}) = 0$ this yields

$$-\int_0^T \int_0^\varrho v\eta_t - \int_0^\varrho v(0)\eta(0) + \int_0^T \int_0^\varrho w_x\eta_x = 0, \tag{8}$$

hence $v_t = w_{xx}$ is satisfied in the weak sense. Defining $u(x,t) := \mu(t) + \int_0^x v(y,t)\mathrm{dy}$ we get easily

$$u_x = v.$$

Choosing μ such that $\int_0^\varrho u(t)$ is constant a simple calculation yields

$$u_t = w_x$$

from (8). For u being periodic we have to assume that $\int_0^\varrho v(0) = 0$ that is the initial data u_0 for $u(0)$ is periodic. Observe that (8) implies $\frac{\mathrm{d}}{\mathrm{dt}} \int_0^\varrho v = 0$.
Since $w \in g(v) = g(u_x)$ we get for all $h \in I\!R$

$$G(h) - G(u_x) \geq w(h - u_x).$$

Therefore for periodic $\eta \in \mathrm{L}^2(0,\mathrm{T};\mathrm{H}^{1,2}(0,\varrho))$ we get

$$\begin{aligned} \int_0^T \int_0^\varrho G(\eta_x) - G(u_x) &\geq \int_0^T \int_0^\varrho w(\eta - u)_x = \\ &= -\int_0^T \int_0^\varrho w_x(\eta - u) = \int_0^T \int_0^\varrho u_t(u - \eta), \end{aligned} \tag{9}$$

hence u is the unique solution of (2.1.3) with initial data u_0 given up to a constant by q_i and $s_{i,0}$.

The conclusion of this subsection is that for any periodic, faceted Γ_0 , which is admissible in the sense of (4), we can construct the solution of (2.1.3) through solving the system of ordinary differential equations (6) for a short time. For this time the solution remains faceted, but if the initial data admits slopes which do not occur in the Wulff-shape they do not disappear instantly. So far the information we obtain by the above construction is only for a limited time. In the next subsection we will extend our construction to get a representation for all time.

2.3 Continuation for all time

We investigate the solution u, v, w on $[0, t_0[$ constructed in the previous subsection for $t \uparrow t_0 < \infty$. We know that the solution u exists on $[0,\infty[$ and $u \in \mathrm{C}^0([0,\infty[, \mathrm{L}^2(0,\varrho))$, especially

$$u(t) \to u(t_0) \quad \text{strongly in } \mathrm{L}^2_{\mathrm{loc}}(I\!R) \text{ for } \mathrm{t} \to \mathrm{t}_0. \tag{1}$$

To extend our representation in the manner of (2.2) it suffices to show that $u(t_0)$ is faceted and admissible in the sense of (2.2.4). We are then able to set up a new system of ordinary differential equations and continue our solution for a short time. Indeed, we will show that $u(t_0)$ has fewer facets than $u(t)$ for $t < t_0$, therefore the construction of (2.2) will give in a finite number of stages a representation of u on $[0, \infty[$.

We know

$$u_x(.,t) = q_i \quad \text{on }]s_{i-1}(t), s_i(t)[.$$

s_i satisfies the following system of ordinary differential equations

$$\begin{aligned} s_i'(t) &= \tfrac{\sigma_i}{\Delta_i(s_i - s_{i-1})} - \tfrac{\sigma_{i+1}}{\Delta_i(s_{i+1} - s_i)}, \\ s_i(0) &= s_{i,0}, \end{aligned} \tag{2}$$

where $\sigma_i := \alpha_{q_i,q_{i+1}} - \alpha_{q_{i-1},q_i}$ and $\Delta_i := q_{i+1} - q_i$. Since $\alpha_{q_i,q_{i+1}} \in g(q_i) \cap g(q_{i+1})$ and g is monotone increasing, we get

$$\frac{\sigma_i}{\Delta_i},\ \frac{\sigma_{i+1}}{\Delta_i} \geq 0. \tag{3}$$

If $q_i > q_{i-1}$ then $\alpha_{q_i,q_{i-1}} = \lim\limits_{q \uparrow q_i} g(q)$. Therefore if $q_i > q_{i+1}, q_{i-1}$ then $\sigma_i = 0$. Taking i such that q_i is maximal we conclude that there is an i with $\sigma_i = 0$. From (2) we get

$$s_i' \leq 0,\ s_{i-1}' \geq 0,$$

and

$$s_{i-1,0} \leq s_{i-1}(t) < s_i(t) \leq s_{i,0}.$$

Now for any $j \in \mathbb{Z}$ we can choose $k \in \mathbb{Z}$ such that $i + kn \leq j < i + (k+1)n$ and get, taking into account $s_{i+n} = s_i + \varrho$,

$$s_{i+kn-1,0} \leq s_j(t) \leq s_{i+(k+1)n,0}.$$

Therefore each s_j is bounded, and there is a sequence $t_l \uparrow t_0$ such that

$$s_j(t_l) \to s_j^\infty. \tag{4}$$

This yields

$$v(t_l) \to v^\infty \quad \text{strongly in } \mathrm{L}^2_{\mathrm{loc}}(\mathbb{R}),$$

where $v^\infty(x) := q_i$ for $s_{i-1}^\infty < x < s_i^\infty$. As $u(t_l)_x = v(t_l)$ and $u(t_l) \to u(t_0)$ strongly in $\mathrm{L}^2_{\mathrm{loc}}(\mathbb{R})$, we obtain $u(t_0)_x = v^\infty$ and $u(t_0)$ is faceted. Because $[0, t_0[$ is the maximal solution interval for (2), there is a $j \in \mathbb{Z}$ such that $s_{j-1}^\infty = s_j^\infty$, that is at least one facet has disappeared, and $u(t_0)$ has less than n facets.

It remains to show that $u(t_0)$ is admissible, that is (2.2.4) holds. Let $s_{i-1}^\infty < s_i^\infty = \ldots = s_{i+k}^\infty < s_{i+k+1}^\infty$, $k \geq 0$ be an endpoint of a facet of $u(t_0)$. The adjacent slopes are q_i and q_{i+k+1}. We have to show

$$g(q_i) \cap g(q_{i+k+1}) \neq \emptyset. \tag{5}$$

When $k = 0$ this follows directly from (2.2.4).

In case $k \geq 1$ we take $j \in \{i+1, \ldots, i+k\}$. We know $s_j(t_l) - s_{j-1}(t_l) \to 0$. From (2.2.3) we get

$$\begin{aligned} |\alpha_{q_{j+1},q_j} - \alpha_{q_j,q_{j-1}}| &= |w(s_j(t_l), t_l) - w(s_{j-1}(t_l), t_l)| \leq \\ \leq C \parallel w_x(t_l) \parallel_{\mathrm{L}^2(0,\varrho)} |s_j(t_l) - s_{j-1}(t_l)|^{\frac{1}{2}} &\leq C(\Lambda) t_l^{-\frac{1}{2}} |s_j(t_l) - s_{j-1}(t_l)|^{\frac{1}{2}} \to 0, \end{aligned}$$

where we have used (2.1.12). Therefore we obtain

$$\alpha_{q_i,q_{i+1}} = \alpha_{q_{i+1},q_{i+2}} = \ldots = \alpha_{q_{i+k},q_{i+k+1}} \in g(q_i) \cap \ldots \cap g(q_{i+k+1}) \neq \emptyset,$$

which yields (5).

We have proved the following proposition:

Proposition (2.3)
For any periodic, faceted initial data u_0 , which is admissible in the sense of (2.2.4), the solution of the variational inequality (2.1.3) remains faceted and satisfies (2.2.4). Moreover, Wulff curves remain Wulff curves. No facets are created and facets disappear only at a finite number of times. In the intervals between these times of disappearance the endpoints of the facets satisfy a system of ordinary differential equations of the same type as (2.3.2).

Remarks:

(i) In subsection (2.5), we will show that this proposition is valid even if the initial data is not admissible.

(ii) On facets with non-Wulff-shape slopes, we see that w is constant. Hence $u_t = w_x = 0$ in the interior of such facets, and these facets do not move at all.

2.4 Stationary states and asymptotics

We are looking for stationary, that is time independent solutions of (2.1.3) that are periodic, faceted, and satisfy (2.2.4). Then the endpoints of the facets s_i are constant. Since there is at least one i such that $\sigma_i = 0$ in (2.3.2), we conclude from (2.3.2) that u is stationary if and only if all σ_i vanish. In terms of the slopes q_i this is equivalent that there is a $j \in \{1, \ldots, N+1\}$ such that $p_{j-1} \leq q_1, \ldots, q_n \leq p_j$, where $p_1, \ldots, p_N$ are the Wulff-shape slopes, $p_0 := -\infty$ and $p_{N+1} = +\infty$. Therefore the stationary Wulff curves are precisely those whose crystalline curvature as defined in [13] is zero.
Incidentally this gives examples, where the initial data has non-Wulff-shape slopes which remain throughout the whole evolution.

Next we consider the asymptotic behaviour of the solution of Proposition(2.3) as $t \to \infty$. We assume that $t_0 \geq 0$ is the final time at which facets disappear. From the differential system (2.3.2) in $[t_0, \infty[$ we get as above, for $t \geq t_0$,

$$\begin{gathered} |\alpha_{q_{i+1},q_i} - \alpha_{q_i,q_{i-1}}| = |w(s_i(t),t) - w(s_{i-1}(t),t)| \leq \\ \leq C \parallel w_x(t) \parallel_{\mathrm{L}^2(0,\varrho)} |s_i(t) - s_{i-1}(t)|^{\frac{1}{2}} \leq C(\Lambda)\varrho^{\frac{1}{2}} t^{-\frac{1}{2}} \to 0 \end{gathered}$$

Therefore $\alpha_{q_{i+1},q_i} = \alpha_{q_i,q_{i-1}}$ and all $\sigma_i = 0$. Moreover, we can bound t_0 . From (2.2.1), we conclude that if $\alpha_{q_{i+1},q_i} \neq \alpha_{q_i,q_{i-1}}$ then $|\alpha_{q_{i+1},q_i} - \alpha_{q_i,q_{i-1}}| = \alpha_j \geq c_0(\gamma)$ for some $j \in \{1, \ldots, N\}$. Therefore the above computation yields

$$t_0 \leq C(\Lambda, \gamma)\varrho^{\frac{1}{2}}. \tag{1}$$

Together with the above discussion we conclude that solutions of Proposition(2.3) attain after a finite time a stationary state, and this time is uniformly bounded for faceted initial data bounded in $\mathrm{C}^{0,1}$.

2.5 The admissibility condition

In this subsection we finally want to remove the admissibility condition (2.2.4), that is

$$g(q_i) \cap g(q_{i+1}) \neq \emptyset \tag{1}$$

for two adjacent slopes q_i and q_{i+1} . As already pointed out in (2.2) it is violated if and only if there are Wulff-shape slopes strictly between q_i and q_{i+1} , more precisely, if $q_i < q_{i+1}$ this means

$$p_{j-1} \leq q_i < p_j < \ldots < p_{j+k} < q_{i+1} \leq p_{j+k+1} \tag{2}$$

for some $j \in \{1, \ldots, N\}$ and $k \geq 0$. We will prove that in this case the evolution instantly creates facets with slopes $p_j, \ldots, p_{j+k}$ between the facet i and $i+1$. Obviously, after this creation the evolving curves are admissible, and Proposition (2.3) applies.
We give two heuristical reasons why exactly these Wulff-shape slopes are inserted. Firstly, if $q_{i-1} < q_i = p_j < q_{i+1}$ then $\sigma_i \neq 0$, where σ_i is defined in (2.3.2). Secondly, if $s_i(t) - s_{i-1}(t) \to 0$ as $t \to t_0$, then, as already computed in (2.3),

$$\begin{gathered} |\sigma_i| = |\alpha_{q_{i+1},q_i} - \alpha_{q_i,q_{i-1}}| = |w(s_i(t),t) - w(s_{i-1}(t),t)| \leq \\ \leq C \parallel w_x(t) \parallel_{\mathrm{L}^2(0,\varrho)} |s_i(t) - s_{i-1}(t)|^{\frac{1}{2}} \leq Ct^{-\frac{1}{2}} |s_i(t) - s_{i-1}(t)|^{\frac{1}{2}} \to 0, \end{gathered}$$

that is $\sigma_i = 0$. Therefore a facet can only disappear when its corresponding $\sigma_{\ldots}$ in the differential system (2.3.2) vanishes.

When the initial data is not admissible, we cannot define w as in (2.2.3). Therefore we introduce hidden facets of length zero with the respective Wulff-shape slopes as in (2) between two facets which are not admissible. Then we can set up the differential system (2.3.2), but now our initial data satisfy only $s_{i,0} \geq s_{i-1,0}$. Nevertheless we know from the above remark, that

$$s_{i,0} = s_{i-1,0} \Rightarrow \sigma_i \neq 0. \tag{3}$$

We will solve (2.3.2) when $s_{i,0} > s_{i-1,0}$ is replaced by (3). We define $l_i := s_i - s_{i-1}$ and conclude from (2.3.2)

$$l_i' = (\frac{\sigma_i}{\Delta_i} + \frac{\sigma_i}{\Delta_{i-1}})\frac{1}{l_i} - \frac{\sigma_{i+1}}{\Delta_i}\frac{1}{l_{i+1}} - \frac{\sigma_{i-1}}{\Delta_{i-1}}\frac{1}{l_{i-1}}.$$

From (2.3.3) we get, choosing Λ large enough, for $\sigma_i \neq 0$

$$\Lambda^{-1} \leq \frac{\sigma_i}{\Delta_i},\ \frac{\sigma_i}{\Delta_{i-1}} \leq \Lambda. \tag{4}$$

We prove the following lemma.
Lemma 1:
We consider $2 \leq n \leq \Lambda,\ \mu > 0,\ 0 < t_1 < t_0$ which satisfy

(a) If $\sigma_i = 0$ then $l_i(0) \geq 2\mu$ and $\forall 0 \leq t \leq t_1 : l_i(t) \geq \mu$.

(b) There is an i with $\sigma_i = 0$ and $l_i(t_1) = \mu$.

Then

$$t_1 \geq c_0(\Lambda)\mu^2$$

and

$$\forall i :\ \forall 0 \leq t \leq t_1 :\quad \begin{aligned} l_i(t) &\geq c_0(\Lambda)\alpha t^{\frac{1}{2}}, \\ |s_i'(t)| &\leq \tfrac{C(\Lambda)}{\alpha} t^{-\frac{1}{2}}, \end{aligned}$$

where $\alpha = \min(\frac{\mu}{\sqrt{t_1}}, 1)$.

Proof:

For $1 \le k \le n$ we define $l_{i,k} := \sum_{j=i}^{i+k-1} l_j$ and get from (2.3.2)

$$l'_{i,k} = s'_{i+k-1} - s'_{i-1} = \frac{\sigma_{i+k-1}}{\Delta_{i+k-1}} \frac{1}{l_{i+k-1}} + \frac{\sigma_i}{\Delta_{i-1}} \frac{1}{l_i} - \frac{\sigma_{i+k}}{\Delta_{i+k-1}} \frac{1}{l_{i+k}} - \frac{\sigma_{i-1}}{\Delta_{i-1}} \frac{1}{l_{i-1}}.$$

Therefore

$$\sigma_i, \ldots, \sigma_{i+k-1} \neq 0 \tag{5}$$

implies with (4)

$$l'_{i,k} \ge \frac{c_0(\Lambda)}{l_{i,k}} - \frac{C(\Lambda)}{l_{i+k}} - \frac{C(\Lambda)}{l_{i-1}}. \tag{6}$$

We prove several assertions, where always (5) and $0 < \beta_0 \le 1$ is assumed.

(i) If $l_{i-1}(t),\ l_{i+k}(t) \ge \beta_0\sqrt{t}$ for all $t \in [0, t_1]$, then $l_{i,k}(t) \ge c_0(\Lambda)\beta_0\sqrt{t}$ for all $t \in [0, t_1]$.

Proof:

For any $0 < \beta \le 1$ we have $\lim_{t \downarrow 0}(l_{i,k}(t) - \beta\sqrt{t}) = s_{i+k-1,0} - s_{i-1,0} > 0$. Suppose there is $\tilde{t} \in [0, t_1]$ such that $\forall 0 \le t \le \tilde{t}:\ l_{i,k}(t) \ge \beta\sqrt{t}$ and $l_{i,k}(\tilde{t}) = \beta\sqrt{\tilde{t}}$. Then (5) and (6) imply

$$0 \ge l'_{i,k}(\tilde{t}) - \frac{\beta}{2}\tilde{t}^{-\frac{1}{2}} \ge \tilde{t}^{-\frac{1}{2}}(\frac{c_0(\Lambda)}{\beta} - \frac{C(\Lambda)}{\beta_0} - \frac{\beta}{2}),$$

hence

$$\beta \ge c_0(\Lambda)\beta_0.$$

//

(ii) If $k \ge 2$ and $l_{i-1}(t),\ l_{i,k}(t) \ge \beta_0\sqrt{t}$ for all $t \in [0, t_1]$, then $l_{i,k-1}(t) \ge c_0(\Lambda)\beta_0\sqrt{t}$ for all $t \in [0, t_1]$.

Proof:

Again for any $0 < \beta \le 1$ we have $\lim_{t \downarrow 0}(l_{i,k-1}(t) - \beta\sqrt{t}) > 0$. Suppose there is $\tilde{t} \in [0, t_1]$ such that $\forall 0 \le t \le \tilde{t}:\ l_{i,k-1}(t) \ge \beta\sqrt{t}$ and $l_{i,k-1}(\tilde{t}) = \beta\sqrt{\tilde{t}}$. We assume $\beta \le \frac{\beta_0}{2}$ and get $l_{i+k-1}(\tilde{t}) \ge \frac{\beta_0}{2}\sqrt{\tilde{t}}$. (5) and (6) yield

$$0 \ge l'_{i,k-1}(\tilde{t}) - \frac{\beta}{2}\tilde{t}^{-\frac{1}{2}} \ge \tilde{t}^{-\frac{1}{2}}(\frac{c_0(\Lambda)}{\beta} - \frac{C(\Lambda)}{\beta_0} - \frac{\beta}{2}),$$

hence

$$\beta \ge c_0(\Lambda)\beta_0.$$

//

(iii) If $l_{i-1}(t),\ l_{i,k}(t) \ge \beta_0\sqrt{t}$ for all $t \in [0, t_1]$, then $l_i(t) \ge c_0(\Lambda)\beta_0\sqrt{t}$ for all $t \in [0, t_1]$.

Proof:

If $k = 1$ then $l_i(t) = l_{i,k}(t) \ge \beta_0\sqrt{t}$.

Now we assume $2 \le k \le n$. From (ii) we get

$$l_{i,k-1}(t) \ge c_0(\Lambda)\beta_0\sqrt{t},$$

and from (iii) for $k-1$ we get

$$l_i(t) \ge c_0(\Lambda)\beta_0\sqrt{t}.$$

//

(iv) If $l_{i-1}(t),\ l_{i+k}(t) \geq \beta_0\sqrt{t}$ for all $t \in [0,t_1]$, then $l_i(t) \geq c_0(\Lambda)\beta_0\sqrt{t}$ for all $t \in [0,t_1]$.
This follows from (i) and (iii).

//

(v) If $l_{i-1}(t),\ l_{i+k}(t) \geq \beta_0\sqrt{t}$ for all $t \in [0,t_1]$, then $l_i(t), \ldots, l_{i+k-1}(t) \geq c_0(\Lambda)\beta_0\sqrt{t}$ for all $t \in [0,t_1]$.
This follows from (iv) by induction on k .

//

From (a) we get for $0 \leq t \leq t_1$ and $\sigma_i = 0$

$$l_i(t) \geq \mu \geq \alpha\sqrt{t},$$

since $\alpha = \min(\frac{\mu}{\sqrt{t_1}}, 1)$. Then (v) implies

$$\begin{array}{rc} \forall i:\ \forall t \in [0,t_1]: & l_i(t) \geq c_0(\Lambda)\alpha\sqrt{t}, \\ \text{and} & |s_i'(t)|,\ |l_i'(t)| \leq \frac{C(\Lambda)}{\alpha}t^{-\frac{1}{2}}. \end{array}$$

Taking $i \in \mathbb{Z}$ as in (b), we get

$$\mu \leq |l_i(t) - l_i(0)| \leq \int_0^{t_1} \frac{C(\Lambda)}{\alpha}t^{-\frac{1}{2}}\mathrm{dt} = \frac{\mathrm{C}(\Lambda)}{\alpha}\sqrt{\mathrm{t}_1},$$

hence

$$\sqrt{t_1} \geq c_0(\Lambda)\mu\alpha \geq c_0(\Lambda)\mu^2\frac{1}{\sqrt{t_1}},$$

and

$$t_1 \geq c_0(\Lambda)\mu^2.$$

///

For solving (2.3.2) with (3) instead of $s_{i,0} > s_{i-1,0}$ we choose $s_{i,0}^\delta \to s_{i,0}$ with $s_{i,0}^\delta > s_{i-1,0}^\delta$ and $s_{i+n,0}^\delta = s_{i,0}^\delta + \varrho$. We denote the solution of (2.3.2) with initial data $\{s_{i,0}^\delta\}$ by s_i^δ and let $[0, t_0^\delta[$ be the maximal interval where this solution exists. For δ small we have for $\sigma_i = 0$

$$s_{i,0}^\delta - s_{i-1,0}^\delta \geq \frac{1}{2}\min_{i,\ \sigma_i=0}(s_{i,0} - s_{i-1,0}) =: 2\mu > 0.$$

We have only to consider the case when there is a j with $s_{j,0} = s_{j-1,0}$. Then $\sigma_j \neq 0$ and $\{s_i^\delta\}$ do not remain stationary, hence according to (2.4) $t_0^\delta < \infty$. Now since t_0^δ is the maximal interval there is an $i \in \mathbb{Z}$ such that $s_i^\delta(t) - s_{i-1}^\delta(t) \to 0$ as $t \uparrow t_0^\delta$. From the above remark we conclude that $\sigma_i = 0$. Therefore the assumptions of Lemma 1 are satisfied, and we get

$$\begin{array}{rc} & t_0^\delta \geq t_1 := c_0(\Lambda)\mu^2, \\ \forall t \in]0,t_1]: & l_i^\delta(t) \geq c_0(\Lambda,\mu)t^{\frac{1}{2}}, \\ & |(s_i^\delta)'(t)| \leq C(\Lambda,\mu)t^{-\frac{1}{2}}. \end{array}$$

This implies that for a subsequence $s_i^\delta \to s_i$ strongly in $C^{0,\frac{1}{4}}([0,t_1])$, and $(s_i^\delta)' \to s_i'$ weakly in $L^2(\tau,t_1)$ for any $\tau > 0$. Moreover

$$s_i(t) - s_{i-1}(t) = l_i(t) \geq c_0(\Lambda,\mu)t^{\frac{1}{2}} \quad \text{for } t \in [0,t_1],$$

and

$$s_i(0) = s_{i,0}.$$

Therefore $s_i(t) > s_{i-1}(t)$ for $t \in]0,t_1]$ and (2.3.2) is satisfied for $t \in]0,t_1]$. Defining u,v,w for $\{s_i\}$ and $\{q_i\}$, we infer from (2.2) that u is a solution of (2.1.3) in $[t,t_1]$ for any $t > 0$. Since $u(t) \to u_0$ strongly in $L^2_{loc}(\mathbb{R})$ as $t \downarrow 0$, u is the unique solution of (2.1.3) with initial data u_0.

2.6 Curved facets

In this subsection, we give an example to show that the evolution according to crystalline curvature is governed by a system of ordinary differential equations which is related to (2.2.6) even if the initial data are not faceted. Some parts of our chosen initial data are smooth curves which are not faceted. Nevertheless our initial data are very restricted, and we will see several limitations of the system of ordinary differential equations for general initial data.

We assume that the real line is subdivided into intervals on which u_0 is either linear with a Wulff-shape slope or $u_0 \in C^1$ and all its slopes lie strictly between two Wulff-shape slopes. We call these intervals curved facets. As in (2.2), we consider $s_i \in C^0([0,t_0[)$ for $i \in \mathbb{Z}$, with $s_{i-1}(t) < s_i(t)$ for $t \in [0,t_0[$, $s_{i+n} = s_i + \varrho$, $n \geq 2$, and define either

$$v(x,t) := q_i \in \{p_1 < \ldots < p_N\} \quad \text{for } s_{i-1}(t) < x < s_i(t),$$

where $\{p_i\}$ are the Wulff-shape slopes, or

$$v(x,t) := u_{0,x}(x) \quad \text{for } s_{i-1}(t) < x < s_i(t).$$

To define w, we first observe that $g(u_{0,x})$ is constant on $]s_{i-1},s_i[$. Hence, assuming the the initial data is admissible, we can define

$$w(s_i(t),t) := \alpha_{i,i+1} \in g(u_{0,x}(s_i(t+))) \cap g(u_{0,x}(s_i(t-))). \tag{1}$$

We extend w to be piecewise-linear in space, and get, setting $\sigma_i := \alpha_{i+1,i} - \alpha_{i,i-1}$,

$$w_x(x,t) = \frac{\sigma_i}{s_i(t) - s_{i-1}(t)} \quad \text{for } s_{i-1}(t) < x < s_i(t). \tag{2}$$

Next we derive the system of ordinary differential equations for $\{s_i\}$ assuming that s_i is differentiable. We choose $s_{i-1}(t) < \beta^- < s_i(t) < \beta^+ < s_{i+1}(t)$. As in (2.2), we get

$$\int_{\beta^-}^{\beta^+} w_{xx}(.,t) = w_x(\beta^+,t) - w_x(\beta^-,t) = \frac{\sigma_{i+1}}{s_{i+1}(t) - s_i(t)} - \frac{\sigma_i}{s_i(t) - s_{i-1}(t)}.$$

For the computation of $\frac{d}{dt}\int_{\beta^-}^{\beta^+} v$, we have to be more careful.

In the case that two Wulff-shape facets meet at $s_{i,0}$, we get as in (2.2)

$$\frac{d}{dt}\int_{\beta^-}^{\beta^+} v = s_i'(t)(q_i - q_{i+1}),$$

hence we obtain (2.2.6) for the derivative of s_i .
Now we assume that at $s_{i,0}$ a Wulff-shape facet on the left side meets a curved facet on the right side. Then we obtain

$$\frac{\mathrm{d}}{\mathrm{dt}} \int_{\beta^-}^{\beta^+} v = s_i'(t)(q_i - u_{0,x}(s_i(t))),$$

and

$$s_i'(t) = \frac{1}{q_i - u_{0,x}(s_i(t))}\left(\frac{\sigma_{i+1}}{s_{i+1}(t) - s_i(t)} - \frac{\sigma_i}{s_i(t) - s_{i-1}(t)}\right).$$

Here we have assumed that $q_i \neq u_{0,x}(s_i(t))$. Indeed, since $u_{0,x}$ are non-Wulff-shape slopes on $]s_{i,0}, s_{i+1,0}[$, we get $\sigma_{i+1} = 0$. Further from the monotonicity of g we get $\frac{-\sigma_i}{q_i - u_{0,x}(s_i)} \geq 0$ when $s_i \geq s_{i,0}$. Then, since $u_{0,x}$ is strictly between two Wulff-shape slopes on $]s_{i,0}, s_{i+1,0}[$, we get $|q_i - u_{0,x}(s_i(t))| \geq c_0$.
If two curved facets meet at $s_{i,0}$, then $\sigma_i = \sigma_{i+1} = 0$ and we get $s_i' = 0$.
The system of ordinary differential equations can be written as

$$\begin{aligned} s_i'(t) &= \frac{1}{\Delta_i(s_i(t))}\left(\frac{\sigma_i}{s_i(t) - s_{i-1}(t)} - \frac{\sigma_{i+1}}{s_{i+1}(t) - s_i(t)}\right), \\ s_i(0) &= s_{i,0}, \end{aligned} \tag{3}$$

where $\Delta_i \in \mathrm{C}^0(I\!R)$, $|\Delta_\mathrm{i}| \geq \mathrm{c}_0$, $\Delta_{\mathrm{i+n}} = \Delta_\mathrm{i}(. - \varrho)$, and $\frac{\sigma_i}{\Delta_i}$, $\frac{\sigma_{i+1}}{\Delta_i} \geq 0$. If a Wulff-shape facet meets a curved facet at $s_{i,0}$, where the Wulff-shape facet is on the left side, then

$$\Delta_i = \frac{1}{u_{0,x} - q_i} \quad \text{on } [s_{i,0}, s_{i+1,0}]. \tag{4}$$

Because of periodicity, (3) has a unique solution on some interval $[0, t_0[$, $0 < t_0 \leq \infty$. From (4) we conclude that $s_{i,0} \leq s_i(t) \leq s_{i+1,0}$ when u_0 is a Wulff-shape facet on $]s_{i-1,0}, s_{i,0}[$ and is a curved facet on $]s_{i,0}, s_{i+1,0}[$. As in (2.2), we compute that $v_t = w_{xx}$. Integrating in space, we obtain $u_x = v$, $u_t = w_x$, and that u is the unique solution of the variational inequality (2.1.3). We see that curved facets can only decrease, but they can be present throughout the whole of the evolution.

Finally, we remark on some of the limitations of the system of ordinary differential equations. We had to assume that the curved facets were C^1 and that their slopes lay strictly between two Wulff-shape slopes in order to get a bounded and continuous functions $\frac{1}{\Delta_i}$. Secondly, we assumed that the initial data could be divided into finitely many facets. If there were infinitely many facets, one would get a infinite system of ordinary differential equations whose solvability is not clear.

3 Numerical Approximation

3.1 Discretization

We consider a discretization of (2.1.3). Let $M \in \mathbb{Z}_+$ be given and set $h = \varrho/M$, where we take $\varrho = 1$ in the remainder of the paper, $i \in \mathbb{Z}$, $x_i = ih$ and $\phi_i(\bullet) \in C(I\!R)$ to be the continuous piecewise linear function satisfying $\phi_i(x_j) = \delta_{ij}$, $j \in \mathbb{Z}$. Let S^h be the space of continuous periodic piecewise linear functions

$$S^h := \{\chi \in C(I\!R) : \ \chi = \sum_j \chi_j \phi_j, \ \chi_{j+M} = \chi_j \ \forall j\}$$

Let $N \in \mathbb{Z}_+$ be given and set $\Delta t = T/N$. Our discrete problem is:-

Given $U^0 \in S^h$, find for $1 \le n \le N$, $U^n \in S^h$ such that

$$(\partial U^n, \chi - U^n)^h + \Phi(\chi) - \Phi(U^n) \ge 0 \quad \forall \chi \in S^h \tag{1}$$

Here we have used the notation

$$\partial U^n := \frac{U^n - U^{n-1}}{\Delta t}$$

$$\Phi(\chi) := \int_0^\rho G(\chi_x) dx$$

and

$$(\chi, \tilde{\chi})^h := \sum_{j=1}^{M} h \chi(x_j) \tilde{\chi}(x_j) \qquad \chi, \tilde{\chi} \in C(I\!R).$$

It follows that

$$\Phi(\chi) = \sum_{j=1}^{M} h G(\frac{\chi_j - \chi_{j-1}}{h}) \qquad \forall \chi \in S^h.$$

The discrete variational inequality (1) is equivalent to

$$\mathcal{E}_n^h(U^n) := \inf_{\chi \in S^h} \mathcal{E}_n^h(\chi) \tag{2}$$

where $\mathcal{E}_n^h(U^n) := \frac{1}{2\Delta t}|\chi - U^{n-1}|_h^2 + \Phi(\chi)$ and $|\bullet|_h = ((\bullet,\bullet)^h)^{1/2}$ is the discrete L^2 norm which satisfies

$$|\chi| \le |\chi|_h \le C|\chi| \qquad \forall \chi \in S^h.$$

Since $\mathcal{E}_n^h(\bullet)$ is a strictly convex continuous functional in S^h problem (1) has a unique solution U^n which satisfies

$$-\partial U_j^n \in \frac{1}{h}(\partial \Phi(U^n))_j \qquad j = 1, ..., M, \tag{3}$$

where $\partial\Phi(\bullet)$ denotes the subdifferential of $\Phi(\bullet)$, see [4].

3.2 An alternative formulation and algorithm

In the next lemma we characterise the subdifferential $\partial\Phi(\chi)$ for $\chi \in S_h$.

Lemma 2:
Let $F(\chi) := \sum_{j=1}^{M} G(\frac{\chi_j - \chi_{j-1}}{h})$ for $\chi \in I\!R^M$ and $\chi_0 = \chi_M$. Then $z \in \partial F(\chi) \subseteq I\!R^M$ if and only if there exists $\eta \in I\!R^M$ such that $\eta_j \in \partial G(\frac{\chi_{j+1} - \chi_j}{h})$ for $j = 0, \ldots, M-1$, $\eta_0 = \eta_M$, and $z_j = \frac{\eta_{j-1} - \eta_j}{h}$ for $j = 1, \ldots, M$.
Proof:
If such an η exists, an easy computation yields that $z \in \partial F(\chi)$.

Now we assume $z \in \partial F(\chi)$. We obtain for any $y \in I\!R^M$, $y_0 = y_M$

$$\sum_{j=1}^{M} (G(\frac{(\chi_j + y_j) - (\chi_{j-1} + y_{j-1})}{h}) - G(\frac{\chi_j - \chi_{j-1}}{h})) = F(\chi + y) - F(\chi) \ge \sum_{j=1}^{M} y_j z_j. \tag{1}$$

For $y = (1, \ldots, 1)$ we observe $F(\chi \pm y) = F(\chi)$, and therefore we get from (1)

$$\sum_{j=1}^{M} z_j = 0.$$

We define $\tilde{\eta}_j := -h \sum_{k=1}^{j} z_k$ for $j = 0, \ldots, M$ and get from the above computations $\tilde{\eta}_0 = \tilde{\eta}_m$ and $z_j = \frac{\tilde{\eta}_{j-1} - \tilde{\eta}_j}{h}$.
Substituting this in (1) and setting $\xi_j := \frac{\chi_j - \chi_{j-1}}{h}$ and $\zeta_j := \frac{y_j - y_{j-1}}{h}$, we obtain

$$\sum_{j=1}^{M} (G(\xi_j + \zeta_j) - G(\xi_j)) \geq \sum_{j=1}^{M} \zeta_j \tilde{\eta}_{j-1}, \tag{2}$$

for all $\zeta \in I\!R^M$ with $\sum_{j=1}^{M} \zeta_j = 0$.
Next we choose $1 \leq i \neq j \leq M$ and set $\zeta_i := -t$, $\zeta_j := t$, and $\zeta_k := 0$ otherwise. Then (2) yields by letting $t \downarrow 0$

$$g(\xi_j +) - g(\xi_i -) \geq \tilde{\eta}_{j-1} - \tilde{\eta}_{i-1}.$$

Hence, there is a $\mu \in I\!R$ such that

$$\forall i, j: \; g(\xi_i -) - \tilde{\eta}_{i-1} \leq \mu \leq g(\xi_j +) - \tilde{\eta}_{j-1}. \tag{3}$$

Defining $\eta_k := \tilde{\eta}_k + \mu$, we get from (3)

$$g(\xi_j -) \leq \eta_{j-1} \leq g(\xi_j +),$$

that is $\eta_{j-1} \in \partial G(\xi_j)$, concluding the proof of the lemma.

///

Applying Lemma 2 to (3.1.3) we obtain the existence of $\{W_j\}$ such that:- for each j

$$\frac{U_j^n - U_j^{n-1}}{\Delta t} = \frac{1}{h}(W_j^n - W_{j-1}^n) \tag{4}$$

and

$$W_j^n \in \partial G(V_j^n), \tag{5}$$

where

$$V_j^n := \frac{U_{j+1}^n - U_j^n}{h} \tag{6}$$

and

$$W_j^n = W_{M+j}^n, \quad V_{M+j}^n = V_j^n. \tag{7}$$

Also we have that for all j

$$V_j^n + \frac{\Delta t}{h^2}(-W_{j-1}^n + 2W_j^n - W_{j+1}^n) = V_j^{n-1}. \tag{8}$$

Clearly $\{U_j^n,\ V_j^n,\ \frac{1}{h}(W_{j-1}^n - W_j^n)\}$ are uniquely defined.

Conversely if $\{V_j^n, W_j^n\}$ satisfy (5), (7) and (8) then we can construct $\{U_j^n\}$ satisfying (4) and (6) by observing that

$$\sum_{j=1}^{M-1} hjV_j^n = MU_M^n - \sum_{j=1}^{M} U_j^n, \qquad \sum_{j=1}^{M} U_j^n = \sum_{j=1}^{M} U_j^{n-1} = \sum_{j=1}^{M} U_j^0$$

yielding

$$U_0^n = U_M^n = h\sum_{j=1}^{M} U_j^0 + \sum_{j=1}^{M-1} h^2 jV_j^n; \quad U_j^n = U_{j-1}^n + hV_{j-1}^n, \qquad j = 1, ..., M. \tag{9}$$

The nonlinear problem (5), (7) and (8) can be written as

$$\underline{v} + \mathbf{A}\underline{w} = \underline{b}, \qquad v_j \in \beta(w_j) \leftrightarrow w_j \in g(v_j) \tag{10}$$

where $\beta(\bullet)$ is a maximal monotone graph and $\mathbf{A}$ is a symmetric positive semi-definite $M \times M$ matrix. We solve this iteratively using a splitting algorithm of Lions–Mercier. Let $\{\underline{v}^0, \underline{w}^0\}$ be given with $\underline{v}^0 \in \beta(\underline{w}^0)$. For fixed $\lambda > 0$ we construct $\{\underline{v}^k, \underline{w}^k\}$ iteratively by solving for $k \geq 0$

$$\underline{w}^{k+1/2} + \lambda\mathbf{A}\underline{w}^{k+1/2} = \underline{w}^k + \lambda(\underline{b} - \underline{v}^k) \tag{11}$$

$$\underline{w}^{k+1} + \lambda\underline{v}^{k+1} = \underline{w}^{k+1/2} + \lambda\underline{v}^k, \qquad \underline{w}_j^{k+1} \in g(v_j^{k+1}). \tag{12}$$

Since we are in finite dimensions we can apply the convergence results of Lions–Mercier [10] to conclude that

$$\lim_{k\to\infty} (\underline{v}^k, \underline{w}^k) = (\underline{v}, \underline{w})$$

which solves (10).

The resolution of (11) requires solving a positive definite circulant system of equations. The resolution of (12) requires the solution of M decoupled equations of the form

$$w + \lambda v = b, \qquad w \in g(v).$$

This is easily achieved by noting that

$$p_1 < p_2 < \ldots < p_N \quad \text{and} \quad l_1 < l_2 < \ldots < l_N$$

where

$$l_i = \sum_{j=1}^{j=i} \alpha_j$$

and setting

$$\begin{array}{ll} r_1 = p_1/\lambda & \\ r_i = (p_i + l_{i-1})/\lambda & i = 2, ..., N \\ \hat{r}_i = (p_i + l_i)\lambda & i = 1, ..., N \end{array}$$

The solution for v can then be obtained from

$$\begin{array}{llll} b \in [r_i, \hat{r}_i] & \Rightarrow \; v = p_i/\lambda & & i = 1, ..., N \\ b \in (\hat{r}_i, r_{i+1}) & \Rightarrow \; v = (b - l_i)/\lambda & \in (p_i, p_{i+1}) & i = 1, ..., N-1 \\ b \in (-\infty, r_1] & \Rightarrow \; v = b/\lambda & & \\ b \in [\hat{r}_N, \infty) & \Rightarrow \; v = (b - l_N)/\lambda & & \end{array}$$

3.3 Convergence

First we derive a bound for $||U_x^n||_\infty$.

Since $g(\bullet)$ is monotone increasing it follows from (3.2.4) that there is a $k \in [1, M]$ such that

$$V_k^n = \max_{1\le j\le M} V_j^n, \qquad W_k = \max_{1\le j\le M} W_j^n.$$

Hence from (3.2.5)

$$V_k^n + \frac{2\Delta t}{h^2} W_k^n \le \max_j V_j^{n-1} + \frac{2\Delta t}{h^2} W_k^n \quad \text{if } k \in [1, ..., M-1].$$

and

$$V_k^n \le \max_j V_j^{n-1}.$$

Similarly we have

$$\min_j V_j^n \ge \min_j V_j^{n-1}.$$

Thus

$$||U_x^n||_\infty \le ||U_x^{n-1}||_\infty.$$

Taking $\chi = U^{n-1}$ in (3.1.1) immediately yields the bound

$$\sum_{n=1}^{N} \Delta t |\partial U^n|_h^2 + \Phi(U^N) \le \Phi(U^0).$$

Taking $\chi = U^n \pm 1$ in (3.1.1) yields the conservation property,

$$(U^n, 1)^h = (U^0, 1)^h.$$

Let u_0 be Lipschitz-continuous with $||u_0||_{C^{0,1}} \le K$ and set $U^0 = \Pi^h u_0$, where $\Pi^h : C(I\!R) \to S^h$ is the piecewise linear interpolation operator. It follows from the above bounds that

$$\sum_{j=1}^{N} \Delta t |\partial U^j|_h^2 + ||U^n||_\infty + ||U_x^n||_\infty \le C(K).$$

Set $\hat{u}_{h,\Delta t}(t)$ and $u_{h,\Delta t}(t)$ to be the piecewise linear and constant functions in time such that on $t \in ((n-1)\Delta t, n\Delta t)$

$$\frac{\partial}{\partial t}\hat{u}_{h,\Delta t}(t) := \frac{U^n - U^{n-1}}{\Delta t}, \qquad u_{h,\Delta t}(t) := U^n.$$

It follows that there exists $u \in H^1(0,T;L^2(0,\varrho)) \cap L^\infty(0,T;W^{1,\infty}(0,\varrho))$ such that

$$\frac{\partial \hat{u}_{h,k}}{\partial t} \text{ converges weakly to } \frac{\partial u}{\partial t} \text{ in } L^2(0,T;L^2(0,\varrho))$$

$$u_{h,k} \text{ converges strongly to } u \text{ in } L^2(0,T;L^2(0,\varrho))$$

$$\frac{\partial u_{h,k}}{\partial x} \text{ converges weakly to } \frac{\partial u}{\partial x} \text{ in } L^2(0,T;L^2(0,\varrho))$$

Let η be a smooth test function with period ϱ in space and set

$$\eta_{h,\Delta t} := \Pi^h \eta(t^n) \qquad t \in ((n-1)\Delta t, n\Delta t).$$

From (3.1.11) we have

$$\int_0^T \left(\frac{\partial}{\partial t}\hat{u}_{h,\Delta t}, \eta_{h,\Delta t} - u_{h,\Delta t}\right)^h dt + \int_0^T \Phi(\eta_{h,\Delta t})dt \geq \int_0^T \Phi(u_{h,\Delta t})dt.$$

A standard quadrature result is

$$|(\chi, \tilde{\chi})^h - (\chi, \tilde{\chi})| \leq Ch|\chi|_h||\tilde{\chi}||_{H^1}.$$

Using the strong convergence of $\eta_{h,\Delta t}$, the convergence properties of $\tilde{u}_{h,\Delta t}$ and $u_{h,\Delta t}$, the continuity of Φ and the weak lower semi continuity of Φ yields (2.1.3) in the limit $h, \Delta t \to 0$.

4 Numerical Results

In this section we perform a series of numerical experiments using the discretization described in section 3 to illustrate points concerning the motion, creation and disappearance of facets that were made in section 2. In all examples we take $\varrho = 1$. The Wulff-shape is defined by p_i and α_i, where, unless stated otherwise, for these examples we have

$$\{p_i\} \in [-2, -1,\ 1,\ 2], \qquad \{\alpha_i\} \in [1,\ 1,\ 1,\ 1], \qquad i = 1, ..., 4.$$

The form of this particular Wulff-shape is shown in Figure 1(a). Computations were performed with a wide range of time and space steps. For the results presented in this section we choose a time step 2.5×10^{-5}, a space step,h, of $1/200$ and a tolerance of 10^{-8} in the iterative scheme (3.2.8,9).

4.1 Wulff Curves

4.1.1 Admissible initial data

Here the initial Wulff curve is defined by, see Section 2.2,

$$\{s_i(0)\} = [1/12,\ 3/12,\ 5/12,\ 7/12,\ 9/12,\ 11/12]$$

and

$$\{q_i(0)\} = [-2, -1,\ 1,\ 2,\ 1, -1]$$

which satisfies both the periodicity and admissibility requirements.

We wish to observe, as in theory, that the curve remains a Wulff curve and that

- No new facets are created
- Admissibility is preserved
- A steady state is reached in finite time

The results are shown in Figure 2. In the graphs of u the points marked on the plots indicate the end points of facets. The facets with slopes of ± 2 shrink (whereas the facets of slopes ± 1 are seen to expand) and are eventually seen to disappear at $t = 0.0177$ at which time a steady state is attained.

It is observed in this simulation, and all others performed, that where motion occurs between two facets then at any time only one mesh point will not be equal to the values p_i of those facets.

4.1.2 Inadmissible initial data

We wish to illustrate the fact that missing facets which make the initial data inadmissible are created instantaneously. We use initial data given by

$$\{s_i(0)\} = [0.2,\ 0.2667,\ 0.7335,\ 0.8]$$

$$\{q_i(0)\} = [-2, -1,\ 2, -1]$$

so that Wulff-shape slopes are missing at the points s_2 and s_3. The results are shown in Figure 3. After one time step it can be seen that facets with slope $v = 1$ have been created at s_2 and s_3. The evolution of the solution then proceeds as the example in section 4.1.1, with the solution eventually reaching a steady state at $t = 0.031$.

4.2 Faceted curve with non-Wulff-shape facets

Here the initial data contains facets with slopes which are not in the Wulff-shape.

4.2.1 Admissible initial data

We wish to show that non-Wulff-shape facets

- Can only decrease in size
- May persist in the steady state

Here we use initial data

$$\{s_i(0)\} = [0.05,\ 0.15,\ 0.35,\ 0.45,\ 0.55\ , 0.65,\ 0.85,\ 0.95]$$

$$\{q_i(0)\} = [-2, -1,\ 0,\ 1,\ 2,\ 1,\ 0, -1]$$

So the initial data contains all the Wulff-shape slopes and is admissible but also contains non-Wulff-shape facets with slope 0. The evolution is shown in Figure 4. The facets with slopes ± 2 and 0 are seen to decrease in length at the same speed. Once the facets with slopes at ± 2 disappear at $t = 0.031$ no further evolution is observed, so a steady state has been reached which contains non-Wulff-shape facets.

4.2.2 Inadmissible initial data

This time we take initial data

$$\{s_i(0)\} = [1/12,\ 3/12,\ 5/12,\ 7/12,\ 9/12,\ 11/12]$$

$$\{q_i(0)\} = [-2, -0.5,\ 0.5,\ 2,\ 0.5, -0.5]$$

which is not a Wulff curve and has missing facets with slope -1 at s_1 and s_6 and with slope $+1$ at s_3 and s_4 making the initial data inadmissible. Figure 5 shows the evolution of the problem. As expected facets at s_1, s_3, s_4 and s_6 are instantly created making the the graph admissible. The facets with slopes at ± 2 and the inadmissible facets with slopes at ± 0.5 shrink and eventually these facets all disappear at the same time $t = 0.011$ yielding a steady state graph with facets of slope ± 1.

4.3 Curved Facets

Introduced in Section 2.6 is the notion of curved facets, where some parts of the initial data are smooth curves with slopes which lie between two Wulff-slopes. From Section 2.6 we know that

- No motion occurs where two curved facets meet
- Motion of the end point between two Wulff-shape facets is given by (2.2.6)
- Motion where a Wulff-shape facet meets a curved facet is given by (2.6.3)

In Figure 6 we show an example of initial data with curved facets, where

$$\{s_i(0)\} = [0.05,\ 0.2,\ 0.23,\ 0.3,\ 0.45,\ 0.55,\ 0.58,\ 0.73,\ 0.88,\ 0.95],$$

$$\{q_1,\ q_3,\ q_4,\ q_6,\ q_7,\ q_{10}\} = [-2, -1,\ 1,\ 2,\ 1, -1]$$

are Wulff shape facets and $\{q_2,\ q_5,\ q_8,\ q_9\}$ are curved facets satisfying

$$q_1 < q_2(x) < q_3, \quad q_4 < q_5(x) < q_6, \quad q_{10} < q_8(x), q_9(x) < q_7.$$

Hence the theory of Section 2.6 applies. It can clearly be seen that the curved facets shrink. Also at s_8, where two curved facets meet, no motion occurs. Eventually the curved facets and the facets with slopes ± 2 are seen to disappear and the steady state seen in Figure 2 is attained at $t = 0.01415$.

4.4 More general initial data

Here we consider some examples with initial data not previously considered.

We first choose as initial data a periodic Wulff curve satisfying the admissibility condition. However, the facets are arranged in a less symmetric fashion, with the initial data defined by

$$\{s_i(0)\} = [0.1,\ 0.15,\ 0.175,\ 0.185,\ 0.36,\ 0.46,\ 0.57,\ 0.69,\ 0.715,\ 0.785,\ 0.85,\ 1]$$

$$\{q_i(0)\} = [1,\ 2,\ 1, -1, -2, -1,\ 1, -1, -2, -1,\ 1,\ 2].$$

Once more we see a reduction in the lengths, and eventual disappearance, of the facets at ± 2. In this problem we also see a movement of U_0^n. This is due to the shape of the curve at $x = 0$ resulting in W^n being non-constant at $i = 0$, so from (3.2.4) $U_0^n \neq U_0^{n-1}$. The steady state attained at $t = 0.0134$ is also different to that of Figures 3 and 4, and is shown in the final graph of u in Figure 7.

Figure 8 shows the evolution of initial data which is a variation of that used in Figure 2, the facets with slopes at ± 1 have been replaced with curved facets, whose slopes at the end points are ± 1. So the theory of Section 2.6 does not apply immediately. As can be seen, the curved facets decrease in length. No motion is observed at the points s_1 and s_3 and at the point where two curved facets meet at s_5. Also, due to the symmetry in the problem, no motion is observed between the facets created with slopes ± 1 at s_2. The two curved facets on the left of figures for v shrink faster than the other two and disappear at $t = 0.00375$, while the final two curved facets disappear at $t = 0.0055$. Once only Wulff-shape facets exist the evolution is as before with the facets with slopes ± 2 decreasing and the graph eventually reaching the steady state seen in Figure 2, although with a lateral shift.

Next we consider the smooth initial data, $u(0) = 1 - (5/4\pi)\cos(2\pi x)$. After one time step facets with slopes at $-2, -1,\ 1$ and 2 have clearly formed. As time evolves the facets with these slopes increase in length at the expense of the curved facets, as expected. In the final picture of Figure 9 all the curved facets have disappeared, from this point the behaviour is as before, the facets with slopes ± 2 decrease and disappear and the steady state is reached, although again with a lateral shift.

4.5 Convergence

In this section we take the initial data and Wulff-shape used for the problem in section 4.1.1. and repeat the calculation with different values of h. In all calculations $\Delta t/h^2$ is taken to be $\frac{1}{2}$. Results are presented in Table 1. T is the time at which the steady state is reached. For this problem the results show a convergence to a time of $T = 0.01767$, for the evolution to the steady state.

N	T
100	0.0178
200	0.0177
300	0.01768
500	0.01767

Table 1

In the above simulations it is noted that as the resolution of the problem is improved then the speed and location of the endpoints of the facets also converge.

A further comparison for this particular problem is given in Section 4.7.

4.6 Other Wulff-Shapes

We now perform a computation with the Wulff-shape shown in Figure 1(b), where $\{p_i\} \in [-1,\ 0,\ 1]$ and $\{\alpha_i\} \in [1,\ 2,\ 1]$. Hence the length of one of the facets is greater than the others. From Section 2.4 and the fact that $\int_0^1 v = 0$ since u is periodic we conclude that $v = 0$ is the only steady state for a Wulff shape which includes the slope 0.

We take as initial data the Wulff curve given by

$$\{s_i(0)\} = [0.175,\ 0.275,\ 0.375,\ 0.425,\ 0.475,\ 0.625,\ 0.725,\ 0.775,\ 0.9,\ 1]$$

$$\{q_i(0)\} = [-1,\ 0,\ 1,\ 0,\ 1,\ 0,\ -1,\ 0,\ 1,\ 0]$$

and use the same values of $\Delta t, N$ and h as before. The evolution of this problem is shown in Figure 10. As can be seen in Figure 10 we see similar behaviour as before with facets with slopes ± 1 decreasing in length and disappearing. In the final graph only two facets with non-zero slope remain and these are seen to disappear at $t = 0.009425$.

So far the Wulff-shapes used have contained few facets. In the final example we take a Wulff-shape defined by

$$\{q_i\} \in [-2 + 4(i-1)/51] \qquad \{\alpha_i\} \in [0.04i], \qquad i = 1, ..., 51.$$

The problem is solved with $M = 500$ on the domain $(0, 1)$ using a timestep of 4×10^{-6}. The initial data for u is taken to be a smooth combination of cosine curves. The results are shown in Figure 11. It can be seen that facets are instantaneously created. Then, as expected, the faceted curve evolves with a reduction of the number of facets as time evolves until the constant steady state, $v = 0$ is reached at $t = 0.0254$.

4.7 Ordinary Differential equations

It is possible to compare results of using the numerical scheme in Section 3.2 with results obtained from solving the system of ordinary differential equations for the jump points of the facets, s_i, given by equation (3.2.2). The system is solved using a 4th and 5th order variable step Runge-Kutta method. As points approach one another singularities occur in the system, these singularities

correspond to times when a facet, or facets, disappear and a new system of equations must be formulated to continue the evolution. Numerically we formulate a new system of equations when $\min_i |s_i - s_{i-1}| < 10^{-3}$. It was observed that standard Runge-Kutta library codes may breakdown or integrate through the singularities when $s_i - s_{i-1} = 0$ and some care has to be taken in their use.

Using the same initial data as the example in Section 4.1.1, Figure 12 shows the evolution of the points $s_i,\ i = 1, ..., 6$ in time. These points correspond with those points marked on the graphs for u in Figure 2. Points s_2 and s_5 remain stationary while the pairs of points s_1, s_6 (due to the periodicity) and s_3, s_4 approach one another. The stopping criteria is met for both of these pairs of points when $T = 0.0176$, which compares well with results in Section 4.5.

In a second example we take admissible initial data given by

$$\{s_i(0)\} = [0.1,\ .15,\ 0.45,\ 0.55,\ 0.75,\ 0.8]$$

$$\{q_i(0)\} = [-2, -1,\ 1,\ 2,\ 1, -1]$$

The lengths of the facets with slopes ± 2 are of different lengths, we therefore expect them to disappear at different times. The evolution of the points, $s_i,\ i = 1, ..., 6$, are shown in Figure 13. In the initial phase of the evolution the points s_3 and s_4 approach one another and meet the stopping criteria at $t = 0.0124$, thus the facet with slope $+2$ disappears. A reduced system of ordinary differential equations,$s_i,\ i = 1, ..., 4$, are formulated at this time, with the initial values for s_i and q_i for this system shown on the Figure. The newly defined points s_3 and s_4 now approach one another and meet the stopping criteria at $t = 0.02215$, thus the facets with slope -2 disappears and the steady state is attained. This computation was repeated using the method in Section 3.2, with $N = 500$ and $\Delta t/h^2 = \frac{1}{2}$, which gave disappearance times for the facets with slopes at $+2$ and -2 of $t = 0.01245$ and $t = 0.0225$ respectively.

In the above examples we have used very simple initial data containing only admissible Wulff-shape slopes, consequently the formulation of the ordinary differential equations and their solution is relatively straight forward. However, the problem becomes much more complicated for Wulff-shapes with many facets and for general initial data, where different forms of ordinary differential equation may have to be formulated for different points in the same problem (see section 2.6). It may also be the case that these equations cannot be formulated. There is also the problem that when a facet, or facets, disappear then a new system of equations has to be constructed. This is in contrast to the numerical method we presented in Section 3.2. No modification to the algorithm has been required for any of the different forms of initial data used. Also to change the Wulff-shape requires only a minor modification to the program.

References

[1] Almgren, F., Taylor, J., Wang, L., (1993) Curvature Driven Flows: A Variational Approach, SIAM Journal on Control and Optimization, **31**, pp. 386-438.

[2] Angenant, S., Gurtin, M., (1989) Multiphase Thermomechanics with Interfacial Structure 2. Evolution of an Isothermal Interface, Archive for Rational Mechanics and Analysis, **108**, pp. 323-391.

[3] Chen, Y., Giga, Y., Goto, S., (1991) Uniqueness and Existence of Viscosity Solutions of generalized Mean Curvature Flow Equations, Journal of Differential Geometry, **33**, pp. 749-786.

[4] Ekeland, I., Temam, R., (1976) Convex Analysis and Variational Problems, North-Holland, Amsterdam.

[5] Evans, L.C., Spruck, J., (1991) Motion of level sets by mean curvature I, Journal of Differential Geometry, **33**, No. 3, pp. 635-681.

[6] Fukui, T., Giga, Y., (1996) Motion of a graph by nonsmooth weighted curvature, World Congress of Nonlinear Analysis '92 (ed. V. Lakshmikantham), Walter de Gruyter, Berlin, **170**, pp. 47-56.

[7] Girao, P.M., Kohn, R.V., (1994) Convergence of a crystalline algorithm for the heat equation in one dimension and for the motion of a graph by weighted curvature, Numerische Mathematik, **Vol. 67**, pp. 41-70.

[8] Gurtin, M., (1993) Thermodynamics of evolving phase boundaries in the plane, Clarendon Press, Oxford.

[9] Gurtin, M., Soner, H. M., Souganidis, P. E., (1995) Anisotropic motion of an interface relaxed by the formation of infinitesimal wrinkles, Journal of Differential Equations, **119**, 1, pp. 54-108.

[10] Lions, P.L., Mercier, B., (1979) Splitting algorithms for the sum of two nonlinear operators, SIAM Journal on Numerical Analalysis, **Vol. 16**, pp. 964-979.

[11] Roosen, Taylor, J., (1994) Modeling Crystal Growth in a Diffusion Field Using Fully-Faceted Interfaces, J. Computational Physics, **114**, pp. 113-128.

[12] Taylor, J.E., (1992) Mean curvature and weighted mean curvature, Acta metall. mater., **Vol. 40**, No. 7, pp. 1475-1485.

[13] Taylor, J.E., (1995) Motion of curves by crystalline curvature including triple junctions and boundary points, Differential Geometry, Proceedings of Symposia in Pure Math., American Mathematical Society, **51**, part 1, pp.417-438.

[14] Taylor, J.E., Cahn, J.W., (1993) Linking Anisotropic Sharp and Diffuse Surface Motion Laws via Gradient Flows, Journal of Statistical Physics, **Vol. 77**, Nos. 1/2, pp. 183-197.

[15] Taylor, J.E., Cahn, J.W., Handwerker, C.A., (1992) Geometric Models of Crystal Growth, Acta metall. mater., **Vol. 40**, No. 7, pp. 1443-1474.

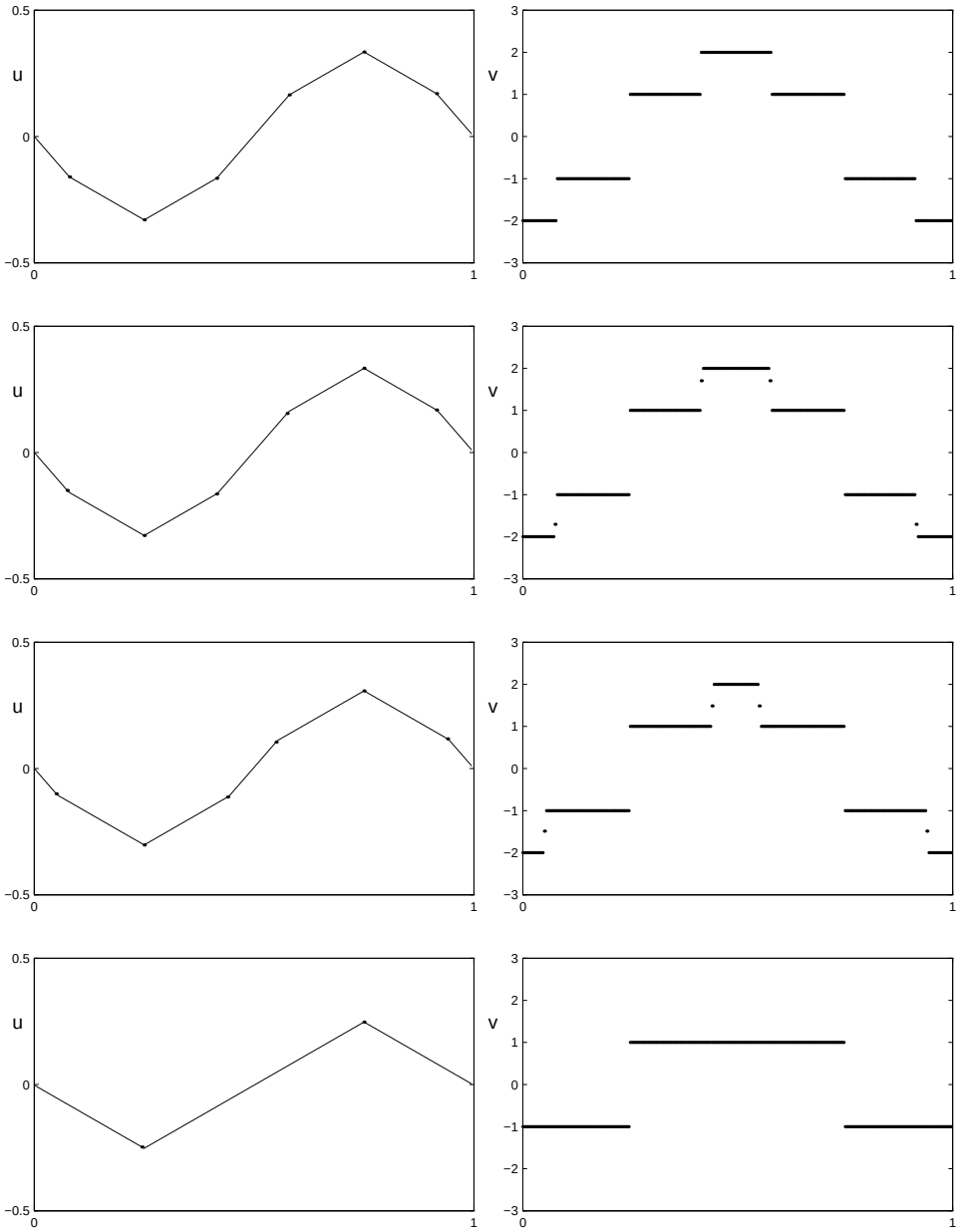

Figure 2: Initial data is an admissible Wulff curve.
u and v are shown at times $t = 0, 0.000025, 0.01, 0.0173$

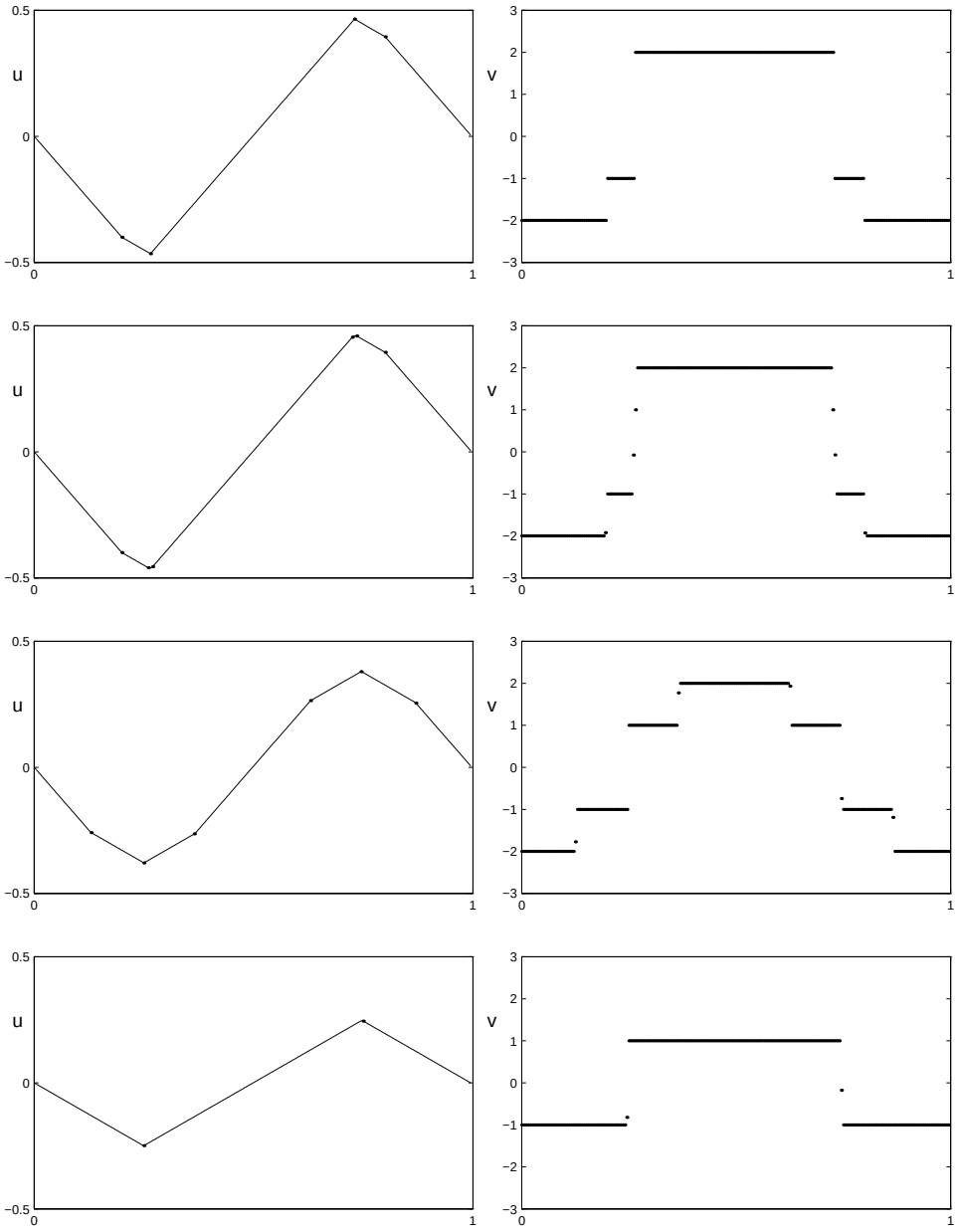

Figure 3: Initial data contains only Wulff-shape facets but is inadmissible. u and v are shown at times $t = 0, 0.0001, 0.0050, 0.0310$

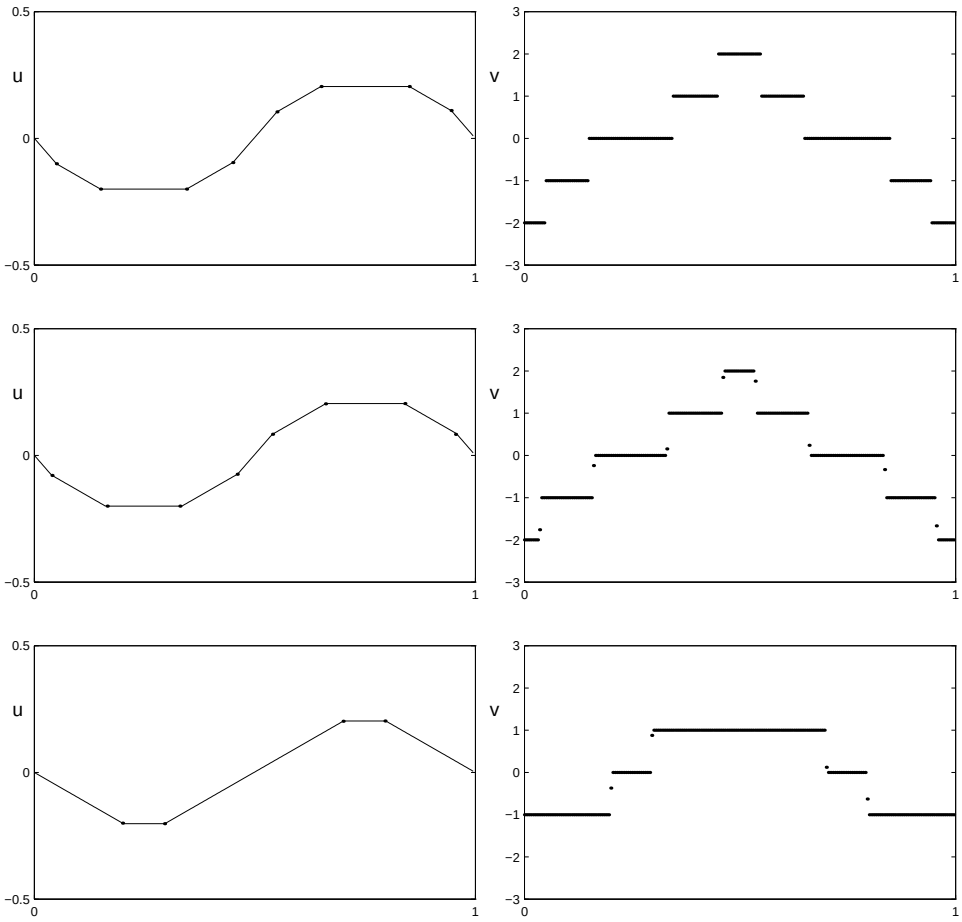

Figure 4: Initial data is an admissible faceted non-Wulff curve. u and v are shown at times $t = 0, 0.0013, 0.00795$

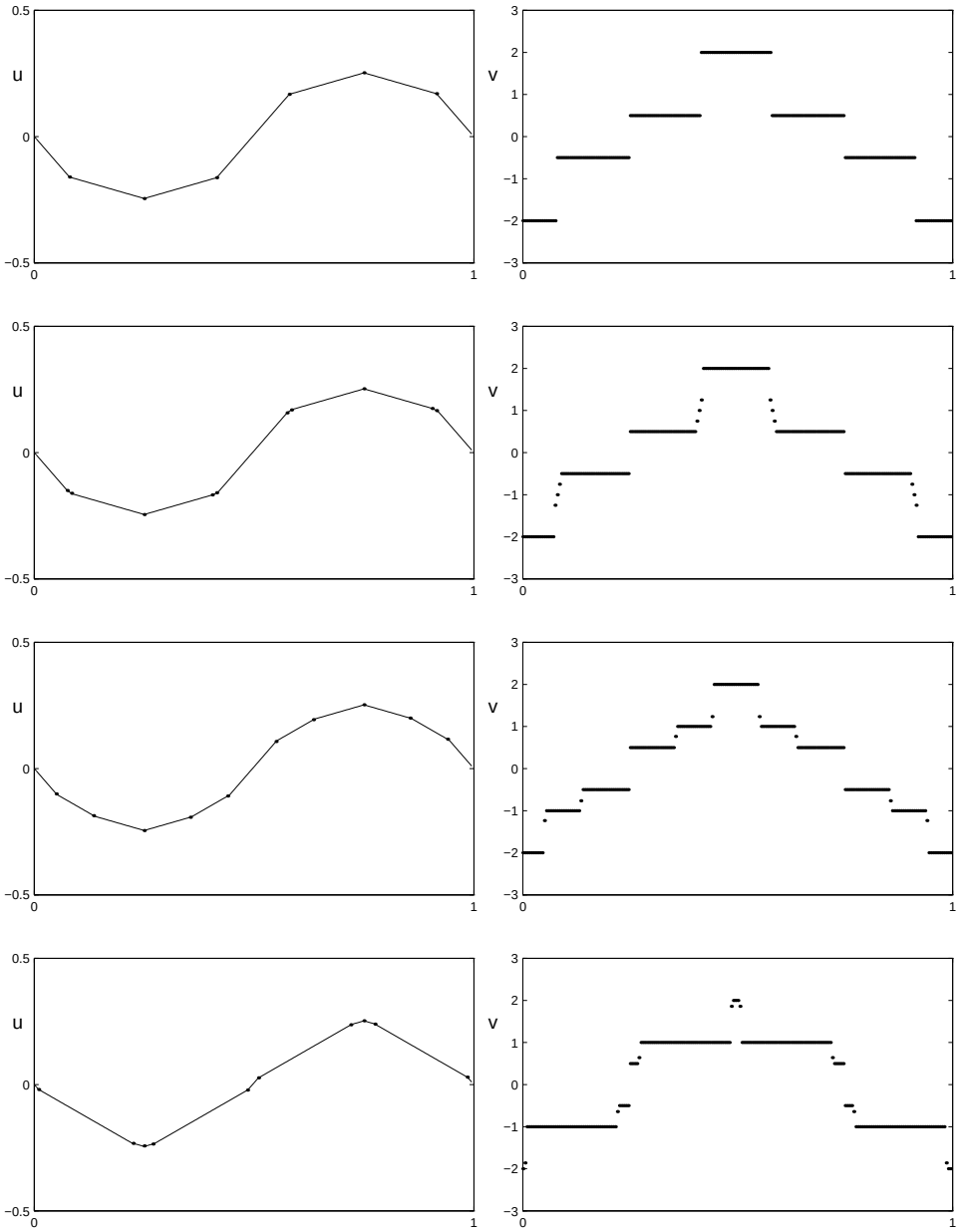

Figure 5: Initial data is a non Wulff curve and is inadmissible. u and v are shown at times $t = 0, 0.000025, 0.00125, 0.0075$

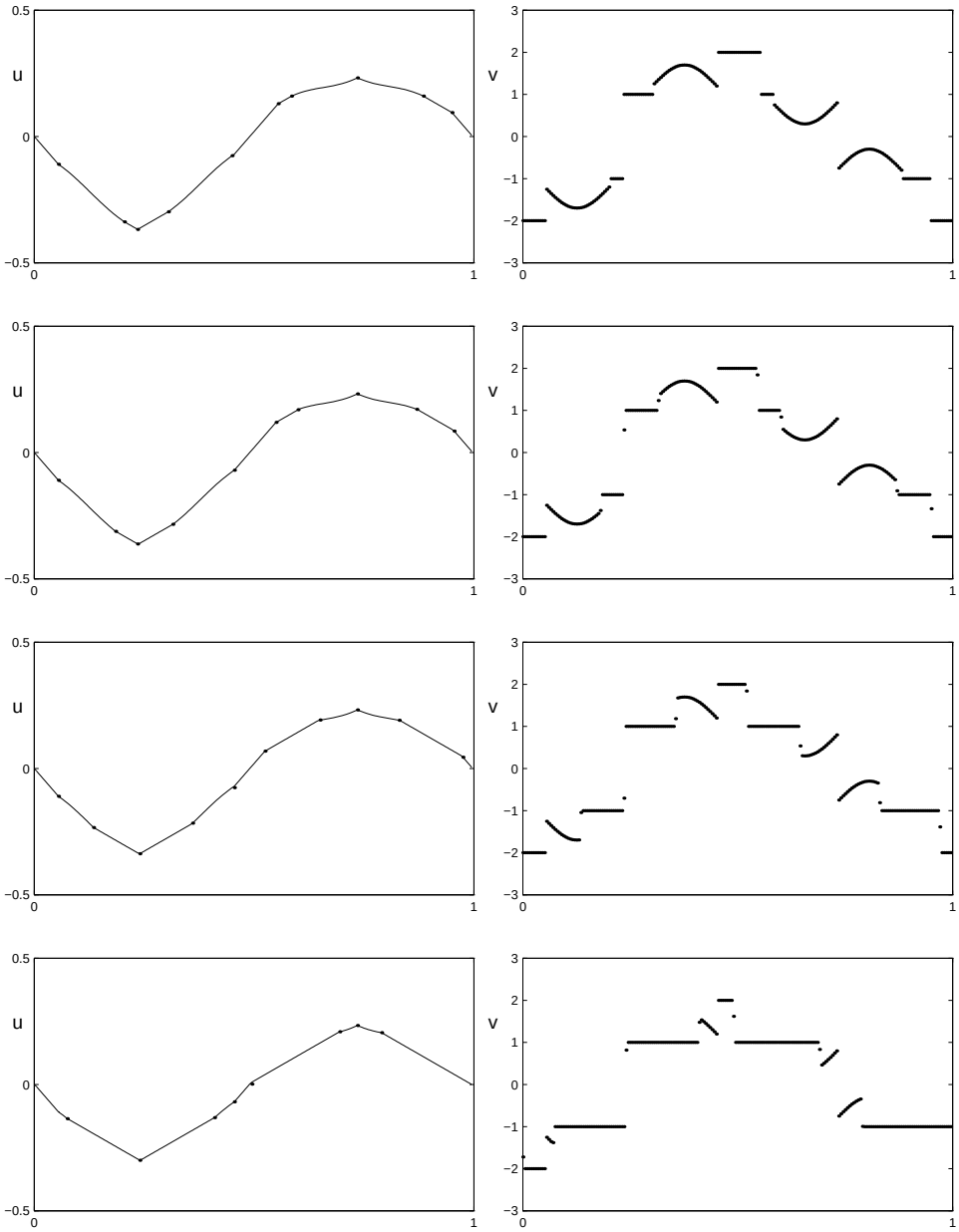

Figure 6: Initial data contains curved facets.
u and v are shown at times $t = 0, 0.000025, 0.00025, 0.00075$

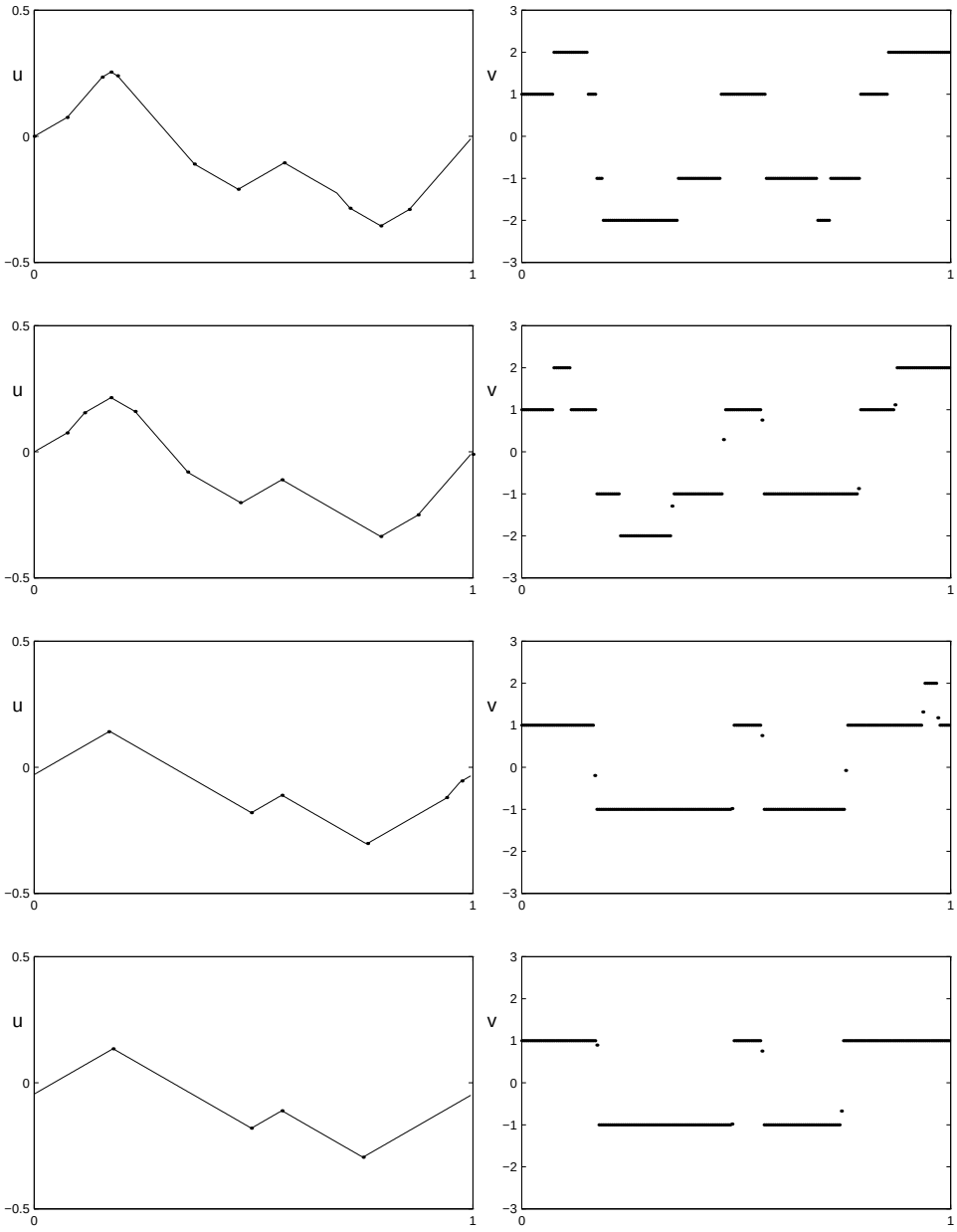

Figure 7: Evolution of an admissible Wulff curve.
u and v are shown at times $t = 0, 0.00025, 0.01, 0.0134$

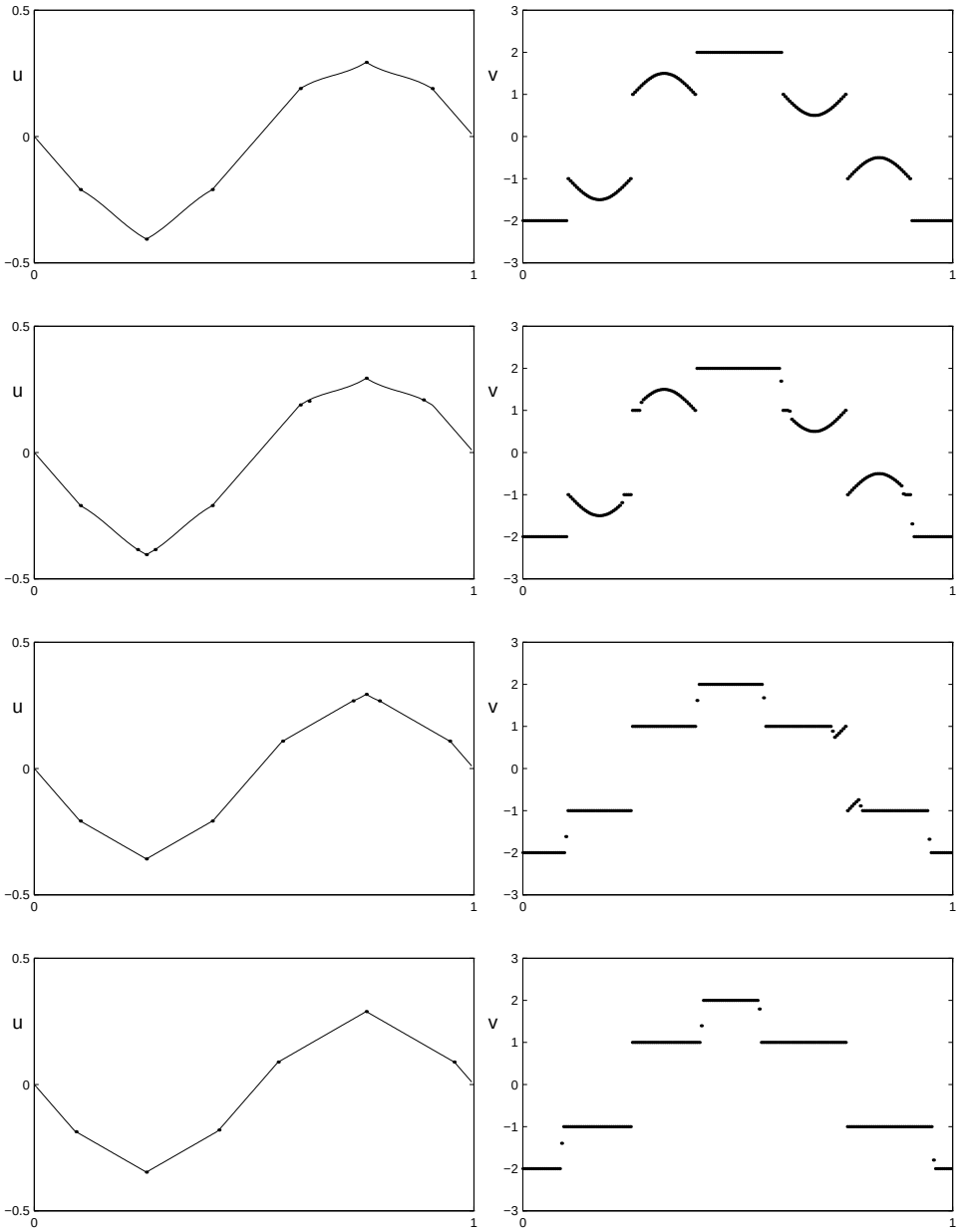

Figure 8: Initial data contains curved facets.
u and v are shown at times $t = 0, 0.000025, 0.00375, 0.0055$

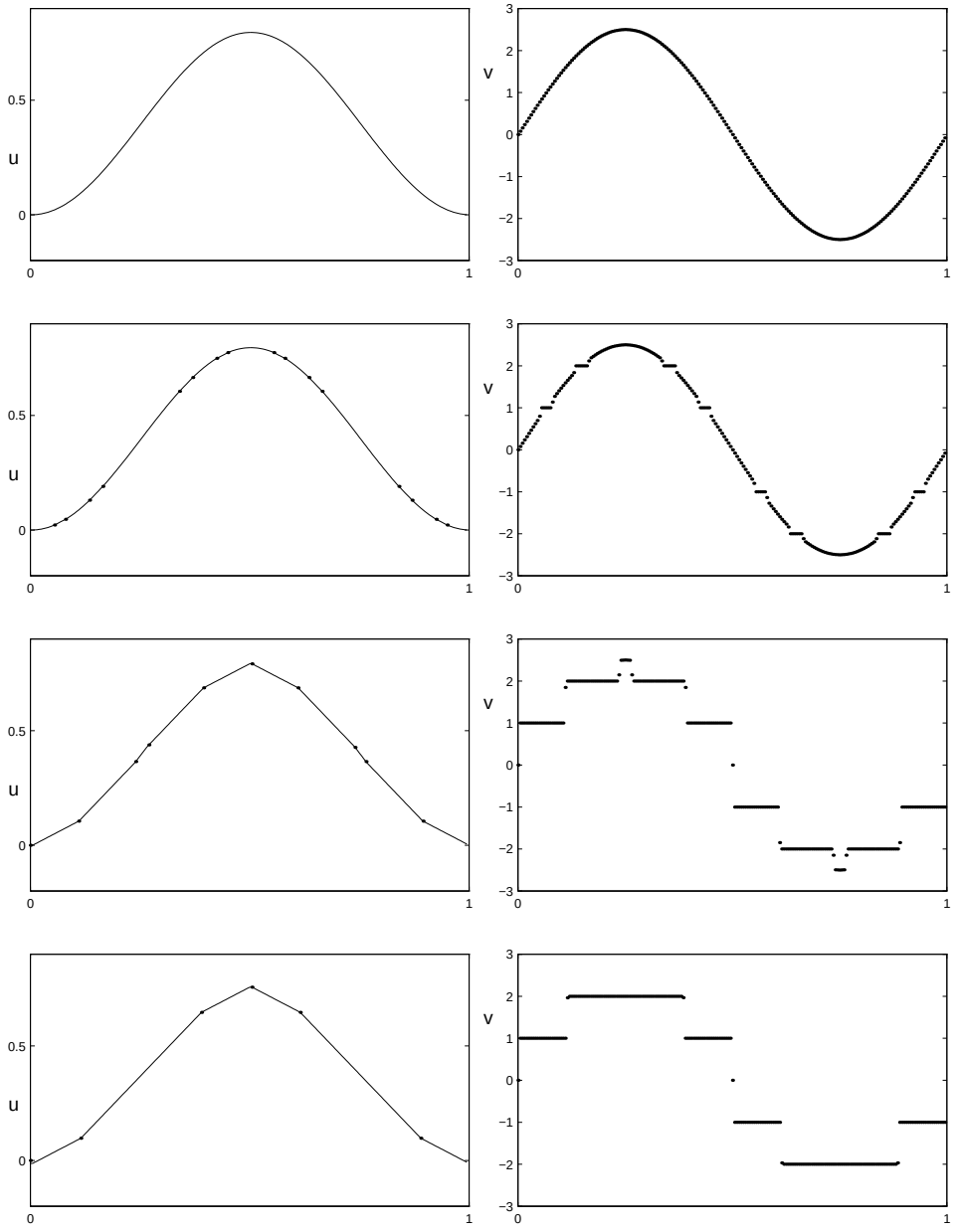

Figure 9: Smooth initial data.
u and v are shown at times $t = 0, 0.000025, 0.00025, 0.00375$

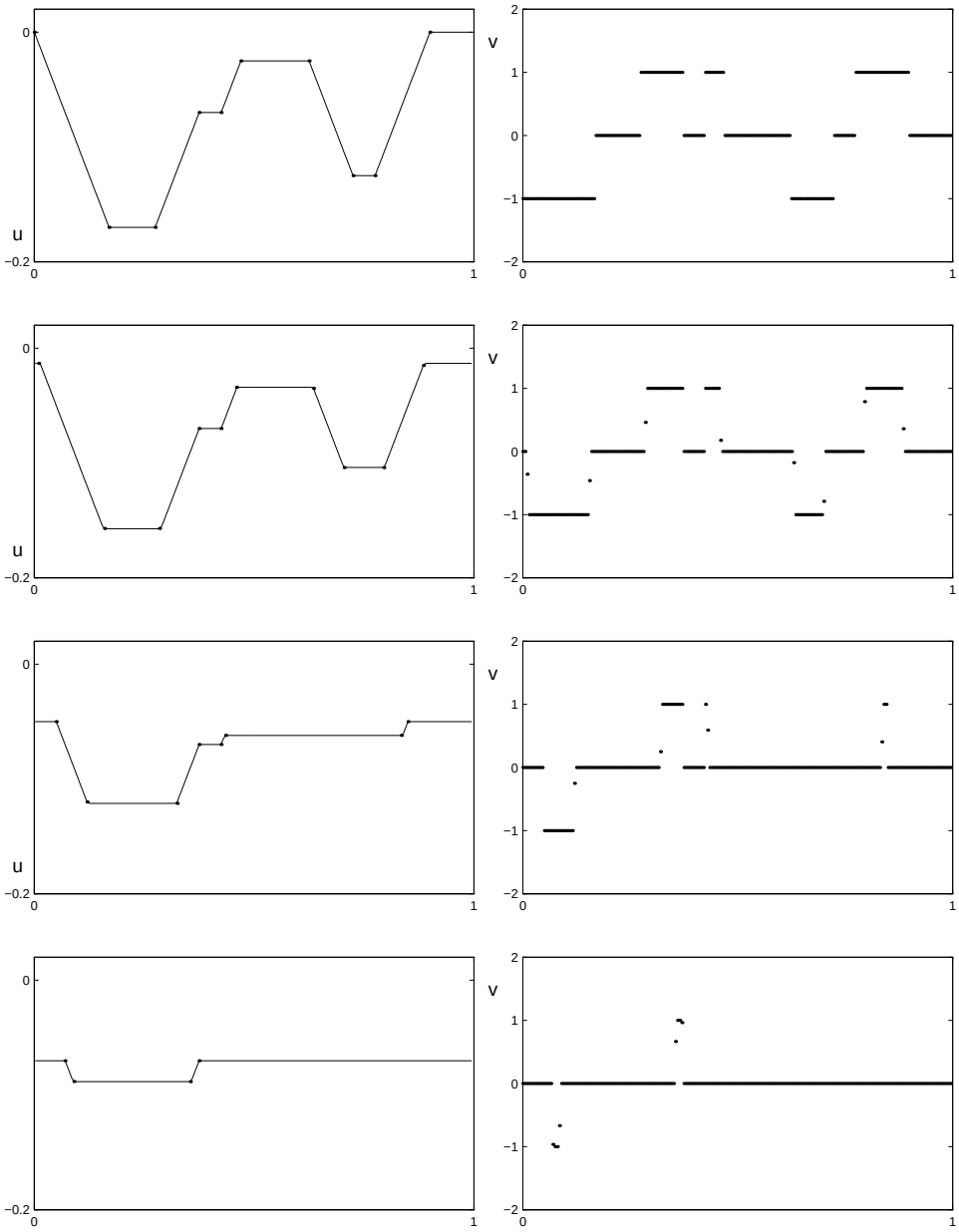

Figure 10: An example of the flow of a Wulff curve for Fig1(b)
u and v are shown at times $t = 0, 0.00075, 0.00375, 0.007625$

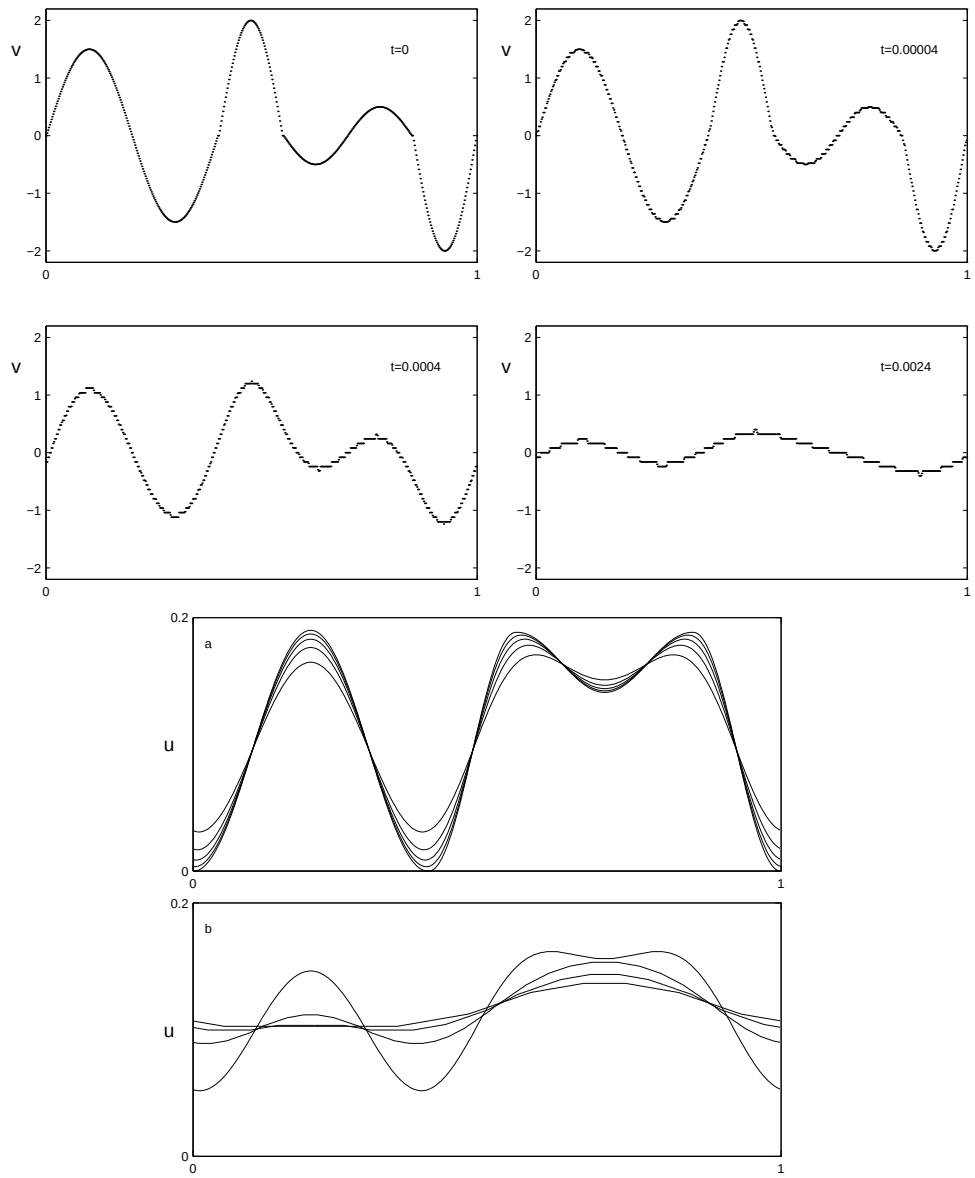

Figure 11: Evolution for a multi-faceted Wulff-shape.
u is shown at times $t = 0, 0.00004, 0.0001, 0.0002, 0.0004$ in a
and $t = 0.0008, 0.0024, 0.004, 0.0056$ in b

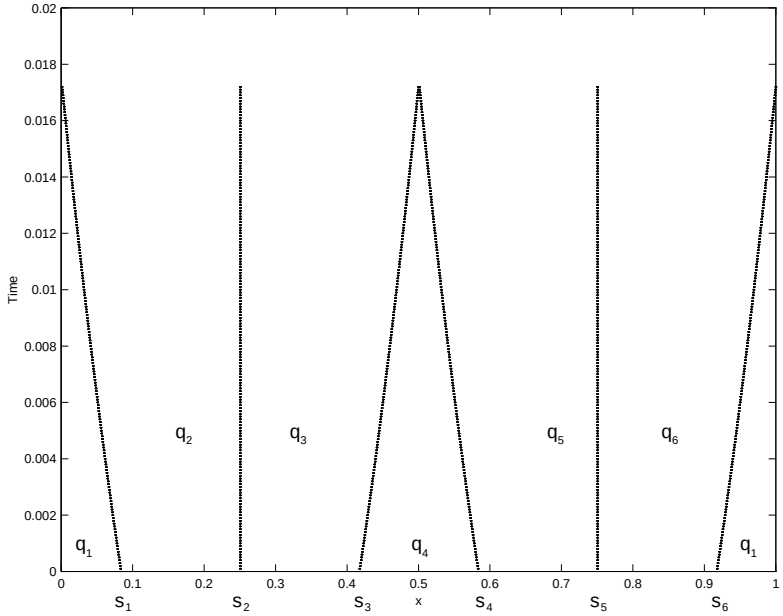

Figure 12: Time evolution of points $s_i, \quad i = 1, ..., 6$ in Figure 1 from solution of ordinary differential equations

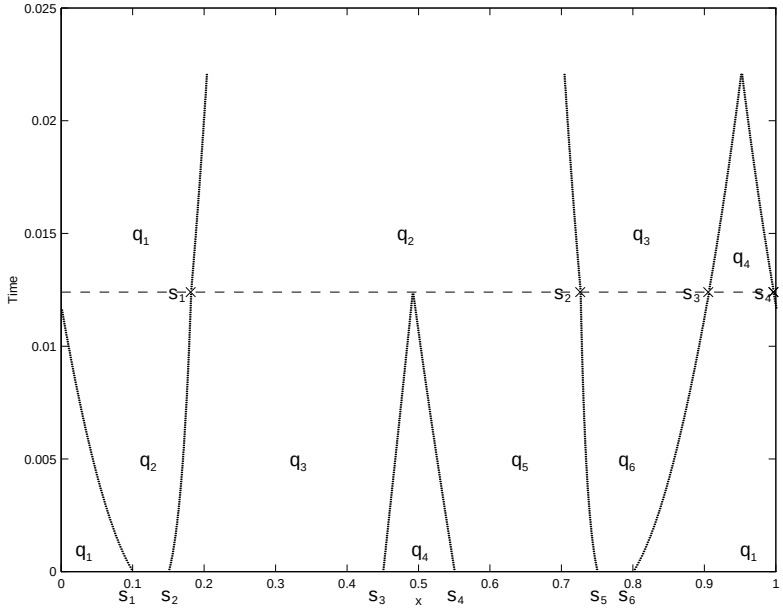

Figure 13: Showing disappearance of facets at different times in the solution of system of ordinary differential equation